# Phospho-Aldol Catalysis via Chiral Schiff Base Complexes of Aluminum†

Julian P. Duxbury, Justin N. D. Warne, Rashfeena Mushtaq, Caroline Ward, Mark Thornton-Pett, Mingliang Jiang, Robert Greatrex, and Terence P. Kee*

*School of Chemistry, University of Leeds, Leeds LS2 9JT, U.K.*

*Received May 5, 2000*

Chiral complexes of aluminum containing the salcyen ligand framework, [(*R*,*R*)-salcyen]-AlX (X = Me, $OSiMe_2{}^tBu$), catalyze the asymmetric addition of diorgano-H-phosphonates to carbonyls: the phospho-aldol reaction. Reaction proceeds smoothly at ambient temperature in various solvents and under aerobic conditions, to afford α-hydroxyphosphonate esters $(MeO)_2P(O)CHR(OH)$, with enantiomeric excesses (ee's) <50%. Although catalyst activity is linked to the nature of X, ee's appear to be only slightly affected. Substitution within the chiral salcyen ligand framework seems to affect ee principally where there is a steric or structural change near the metal center. Although catalysis is tolerant of small quantities of water, excess water leads to attenuation of enantioselectivity through decomposition of catalyst to afford hydrated aluminas which competes through achiral phospho-aldol catalysis. Kinetic analyses reveal a second-order polynomial relationship of the form $x/([A_0] - x)[A_0] = k_2t + k_2t^2$, where $[A_0]$ is the initial concentration of H-phosphonate and carbonyl and $x$ the degree of reaction. This may suggest that the metal complex must first be converted to another, more active precursor prior to catalytic turnover. Hammett analyses suggest that carbonyl binding to the metal center results in enhanced ee's, while single-crystal analyses on four aluminum complexes support the view that twisting of the ligand framework, as measured by the five-coordinate $\tau$ parameter, from a purely meridional geometry may be advantageous to stereoselectivity. Strategies for future developments are discussed in light of the results herein.



## Introduction

Phosphonates (B) have received significant attention in recent years as a result of their ability to mimic biological phosphates (A).[1] Their efficacy results mainly from the stability of phosphonate phosphorus−carbon (P−C) linkages toward cellular enzymes, yet replacing a P−O linkage by a P−C bond obviously leads to differences in character, especially in $pK_a$, hydrogen bonding, and metal binding capacity.[1]

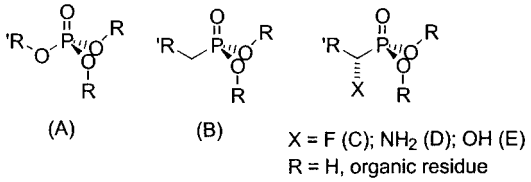


Such differences may be overcome by introducing fluoro (C),[2] amino (D),[3] or hydroxy (E)[4] groups at the α-carbon site to generate α-functionalized phosphonic frameworks with improved phosphate mimicry and/or enzyme inhibition properties. α-Functionality introduces

† The poem *Dr. Faustus' Shirt* is available as a Word 2000 attachment upon e-mail request to t.p.kee@chem.leeds.ac.uk.

(1) Hilderbrand, R. L. *The Role of Phosphonates in Living Systems*; CRC Press: Boca Raton, FL, 1983. Engel, R. *Chem. Rev.* **1977**, *77*, 349. Blackburn, G. M. *Chem. Ind.* **1981**, 134. Krapcho, J.; Turk, C.; Cushman, D. W.; Powell, J. R.; DeForrest, J. M.; Spitzmiller, E. R.; Karanewsky, D. S.; Duggan, M.; Rovnvak, G.; Schwartz, J.; Natarajan, S.; Godfrey, J. D.; Ryono, D. E.; Neubeck, R.; Petrillo, E. W., Jr. *J. Med. Chem.* **1988**, *31*, 1148. Lejczak, B.; Kafarski, P.; Makowiecka, E. *Biochem. J.* **1987**, *242*, 81.

(2) Smyth, M. S.; Ford, H., Jr.; Burke, T. R., Jr. *Tetrahedron Lett.* **1992**, *33*, 4137. Groves, M. R.; Yao, Z. J.; Roller, P. P.; Burke, T. R., Jr.; Barford, D. *Biochemistry* **1998**, *37*, 17773. Stirtan, W. G.; Withers, S. G. *Biochemistry* **1996**, *35*, 15057. Chen, L.; Wu, L.; Otaka, A.; Smyth, M. S.; Roller, P. P.; Burke, T. R., Jr.; Denhertog, J.; Zhang, Z. Y. *Biochem. Biophys. Res. Commun.* **1995**, *216*, 976. Burke, T. R., Jr.; Smyth, M. S.; Nomizu, M.; Otaka, A. Roller, P. P. *J. Org. Chem.* **1993**, *58*, 1336.

(3) Bergin, C.; Hamilton, R.; Walker, B.; Walker, B. J. *Chem. Commun.* **1996**, 1155. Lefebvre, I. M.; Evans, S. A., Jr. *J. Org. Chem.* **1997**, *62*, 7532. Maury, C.; Gharbaoui, T.; Royer, J.; Husson, H.-P. *J. Org. Chem.* **1996**, *61*, 3687. Song, Y.; Niederer, D.; Lane-Bell, P. M.; Lam, L. K. P.; Crawley, S.; Palcic, M. M.; Pickard, M. A.; Pruess, D. L.; Vederas, J. C. *J. Org. Chem.* **1994**, *59*, 5784. Cabella, G.; Jommi, G.; Pagliarin, R.; Sello, G.; Sisti, M. *Tetrahedron* **1995**, *51*, 1817. Ouazzani, F.; Roumestant, M.-L.; Viallefont, P.; El Hallaoui, A. *Tetrahedron: Asymmetry* **1991**, *2*, 913. Chung, S.-K.; Kang, D.-H. *Tetrahedron: Asymmetry* **1996**, *7*, 21. Yokamatsu, T.; Yamagishi, T.; Shibuya, S. *Tetrahedron: Asymmetry* **1993**, *4*, 1401. Maury, C.; Royer, J.; Husson, H.-P. *Tetrahedron Lett.* **1992**, *33*, 6127. Wang, C.-L. J.; Taylor, T. L.; Mical, A. J.; Spitz, S.; Reilly, T. M. *Tetrahedron Lett.* **1992**, *33*, 7667. Bartlett, P. A.; Kezer, W. B. *J. Am. Chem. Soc.* **1984**, *106*, 4282. Bartlett, P. A.; Hanson, J. E.; Giannousis, P. P. *J. Org. Chem.* **1990**, *55*, 6268. Allen, J. G.; Atherton, F. R.; Hall, M. J.; Hassall, C. H.; Holmes, S. W.; Lambert, R. W.; Nisbet, L. J.; Ringrose, P. S. *Nature (London)* **1978**, 272, 56. Copie, V.; Faraci, W. S.; Walsh, C. T.; Griffin, R. G. *Biochemistry* **1988**, *27*, 4966.

(4) Gajda, T. *Tetrahedron: Asymmetry* **1994**, *5*, 1965. Khushi, T.; O'Toole, K. J.; Sime, J. T. *Tetrahedron Lett.* **1993**, *34*, 2375. Yokamatsu, T.; Yoshida, Y.; Shibuya, S. *J. Org. Chem.* **1994**, *59*, 7930. Heisler, A.; Rabiller, C.; Douillard, R.; Goalou, N.; Hägele, G.; Levayer, F. *Tetrahedron: Asymmetry* **1993**, *4*, 959. Yuan, C.; Chen, D. *Synthesis* **1992**, 531. Li, Y.-F.; Hammerschmidt, F. *Tetrahedron: Asymmetry* **1993**, *4*, 109. Meier, C.; Laux, W. H. G. *Tetrahedron: Asymmetry* **1996**, *7*, 89. Blazis, V. J.; Koeller, K. J.; Spilling, C. D. *J. Org. Chem.* **1995**, *60*, 931. Pogatchnik, D. M.; Wiemer, D. F. *Tetrahedron Lett.* **1997**, *38*, 3495.

10.1021/om000386m CCC: $19.00 
Publication on Web 09/30/2000

**Scheme 1**

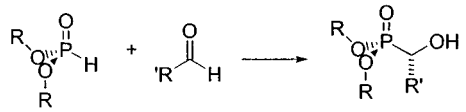

chirality at the α-carbon atom and consequently a stereoisomeric influence upon biological properties.[5] Consequently, there is a growing need to develop new and efficient synthetic routes to α-functionalized phosphonic structures that permit control of stereochemistry. In this contribution we describe our work on one such process, the catalytic asymmetric phospho-aldol (PA) reaction (Scheme 1),[6] an extremely versatile process for the synthesis of α-hydroxyphosphonic systems with biological and medicinal applications; for example, in the inhibition of renin,[7] HIV protease,[8] inositol monophosphatase,[9] and EPSP synthetase.[10]

A key objective of our research program[11] in phosphotransfer chemistry is the development of metal-based catalysts for the PA process. These complexes must be (i) simple to prepare, (ii) inexpensive, (iii) tunable, (iv) compatible with air and water, (v) reusable without extensive reprocessing, and of course (vi) stereoselective.

Existing PA catalysts[6] satisfy the above criteria to varying degrees, but we seek new air- and water-compatible catalysts which, for the first time, move away from binaphthol[6c−k] as the principal source of chiral recognition in this process. Herein we describe our work on a family of chiral organometallic and metallo-organic catalysts that function as effective PA catalysts. Part of this work has appeared in preliminary form.[12]

**Scheme 2**

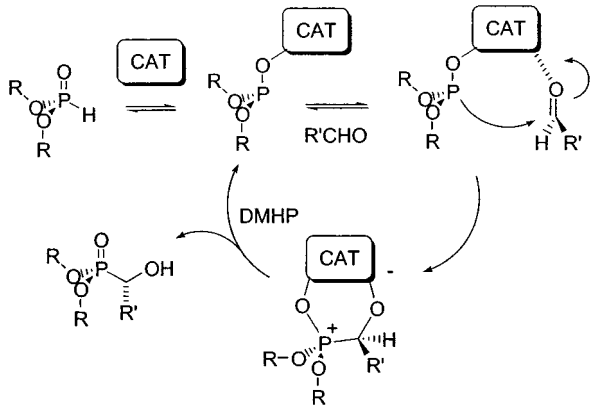


## Results

It has long been recognized that the PA process is base-catalyzed;[6] however, only recently have simple organometallic bases such as diethylzinc been shown to effect clean and rapid catalysis.[11j] A working mechanistic picture for this organometallic-catalyzed PA reaction is summarized in Scheme 2. Initial deprotonation of H-phosphonate by a suitably polarized $M^{\delta+}-C^{\delta-}$ bond (CAT) is followed by P−C bond formation and concluded by proton transfer from H-phosphonate leading to decomplexation of product phosphonate. A logical asymmetric strategy would be to encourage both H-phosphonate and carbonyl to come together in the crucial stereodetermining P−C bond forming step within a chiral catalyst manifold. The problem then becomes one of deciding which chiral manifold best fulfils the criteria outlined above.

The Salen class of Schiff bases is a widely used ligand in coordination chemistry as a result of its ease of synthesis and tunability.[13] Consequently, our interest was engaged by enantiopure derivatives based on the *trans*-1,2-diaminocyclohexyl framework (the Salcyen ligand[14]), championed principally by Jacobsen and others.[13] Of particular interest to us is the extensive and thorough work of Atwood on Schiff base complexes of aluminum alkyls,[15] coupled with earlier observations of Barron[16] that such complexes are far more water-tolerant than many other aluminum alkyls. Our strategy was then 3-fold: (1) to prepare complexes in which a suitably polarized $Al^{\delta+}-X^{\delta-}$ linkage is embedded within a chiral Salen environment, (2) to test their ability as catalysts in the PA process, and (3) to illuminate mechanisms for improving catalyst performance and selectivity.

**Question 1. Aluminum−Salcyen Complexes.** (*R*,*R*)-*N*,*N*′-Bis(salicylimine)-1,2-cyclohexanediamine (Salcyen;

(5) See for example: Kametani, T.; Kigasawa, K.; Hiiragi, M.; Wakisaki, K.; Haga, S.; Sugi, H.; Tanigawa, K.; Suzuki, Y.; Fukawa, K.; Irino, O.; Saita, O.; Yamabe, S. *Heterocycles* **1981**, *16*, 1205. Bayliss, E.; Campbell, C. D.; Dingwall, J. G. *J. Chem. Soc., Perkin Trans. 1* **1984**, 2845.

(6) (a) Wynberg, H.; Smaardijk, A. A. *Tetrahedron Lett.* **1983**, *24*, 5899. (b) Smaardijk, A. A.; Noorda, S.; van Bolhuis, F.; Wynberg, H. *Tetrahedron Lett.* **1985**, *26*, 493. (c) Yokomatsu, T.; Yamagishi, T.; Shibuya, S. *Tetrahedron: Asymmetry* **1993**, *4*, 1779, 1783. (d) Rath, N. P.; Spilling, C. D. *Tetrahedron Lett.* **1994**, *35*, 227. (e) Sasai, H.; Arai, S.; Tahara, Y.; Shibasaki, M. *J. Org. Chem.* **1995**, *60*, 6656. (f) Arai, T.; Bougauchi, M.; Sasai, H.; Shibasaki, M. *J. Org. Chem.* **1996**, *61*, 2926. (g) Yokomatsu, T.; Yamagishi, T.; Matsumoto, K.; Shibuya, S. *Tetrahedron* **1996**, *52*, 11725. (h) Gröger, H.; Saida, Y.; Arai, S.; Martens, J.; Sasai, H.; Shibasaki, M. *Tetrahedron Lett.* **1996**, *37*, 9291. (i) Yokomatsu, T.; Yamagishi, T.; Shibuya, S. *J. Chem. Soc., Perkin Trans. 1* **1997**, 1527. (j) Shibasaki, M.; Sasai, H.; Arai, T. *Angew. Chem., Int. Ed. Engl.* **1997**, *36*, 1236. (k) Groaning, M. D.; Rowe, B. J.; Spilling, C. D. *Tetrahedron Lett.* **1998**, *39*, 5485.

(7) Patel, D. V.; Rielly-Gauvin, K.; Ryono, D. E. *Tetrahedron Lett.* **1990**, *31*, 5587; 5591.

(8) Stowasser, B.; Budt, K.-H.; Jian-Qi, L.; Peyman, A.; Ruppert, D. *Tetrahedron Lett.* **1992**, *33*, 6625.

(9) MacCleod, A. M.; Baker, R.; Hudson, M.; James, K.; Roe, M. B.; Knowles, M.; MacAllister, G. *Med. Chem. Res.* **1992**, *2*, 96.

(10) Shikorski, J. A.; Miller, M. J.; Baccolino, D. S.; Cleary, D. G.; Corey, S. D.; Font, J. L.; Gruys, K. J.; Han, C. Y.; Lin, K. C.; Pansegrau, P. D.; Ream, J. E.; Schnur, D.; Shan, A.; Walker, M. C. *Phosphorus, Sulfur Silicon Relat. Elem.* **1993**, *76*, 115.

(11) (a) Sum, V.; Kee, T. P. *J. Chem. Soc., Perkin Trans. 1* **1993**, 2701. (b) Devitt, P. G.; Kee, T. P. *J. Chem. Soc., Perkin Trans. 1* **1994**, 3169. (c) Sum, V.; Baird, C. A.; Kee, T. P., Thornton-Pett, M. *J. Chem. Soc., Perkin Trans. 1* **1994**, 3183. (d) Cain, M. J.; Baird, C. A.; Kee, T. P. *Tetrahedron Lett.* **1994**, *35*, 8671. (e) Mitchell, M. C.; Cawley, A.; Kee, T. P. *Tetrahedron Lett.* **1995**, *36*, 287. (f) Devitt, P. G.; Kee, T. P. *Tetrahedron* **1995**, *51*, 10987. (g) Whitnall, M. R.; Hii, K. K.; Thornton-Pett, M.; Kee, T. P. *J. Organomet. Chem.* **1997**, *529*, 35. (h) Jones, V. A.; Sriprang, S.; Thornton-Pett, M.; Kee, T. P. *J. Organomet. Chem.* **1998**, *567*, 199. (i) Mitchell, M. C.; Taylor, R. J.; Kee, T. P. *Polyhedron* **1998**, *17*, 433. (j) Davies, S. R.; Mitchell, M. C.; Cain, C. P.; Devitt, P. G.; Taylor, R. J.; Kee, T. P. *J. Organomet. Chem.* **1998**, *550*, 29.

(12) Duxbury, J. P.; Cawley, A.; Thornton-Pett, M.; Wantz, L.; Warne, J. N. D.; Greatrex, R.; Brown, D.; Kee, T. P. *Tetrahedron Lett.* **1999**, *40*, 4403.

(13) Hobday, M. D.; Smith, T. D. *Coord. Chem. Rev.* **1972**, *9*, 311. Serron, S. A.; Haar, C. M.; Nolan, S. P. *Organometallics* **1997**, *16*, 5120. Konsler, R. G.; Karl, J.; Jacobsen, E. N. *J. Am. Chem. Soc.* **1998**, *120*, 10780.

(14) Atwood, D. A. *Coord. Chem. Rev.* **1997**, *165*, 267.

(15) Atwood, D. A.; Jegier, J. A.; Rutherford, D. *Inorg. Chem.* **1996**, *35*, 63. Atwood, D. A.; Gabbai, F. P.; Lu, J.; Remington, M. P.; Rutherford, D.; Sibi, M. P. *Organometallics* **1996**, *15*, 2308. Jegier, J. A.; Atwood, D. A. *Inorg. Chem.* **1997**, *36*, 2034. Atwood, D. A.; Hill, M. S.; Jegier, J. A.; Rutherford, D. *Organometallics* **1997**, *16*, 2659.

(16) Gurian, P. L.; Cheatham, L. K.; Ziller, J. W.; Barron, A. R. *J. Chem. Soc., Dalton Trans.* **1991**, 1449.

**Scheme 3**[a]

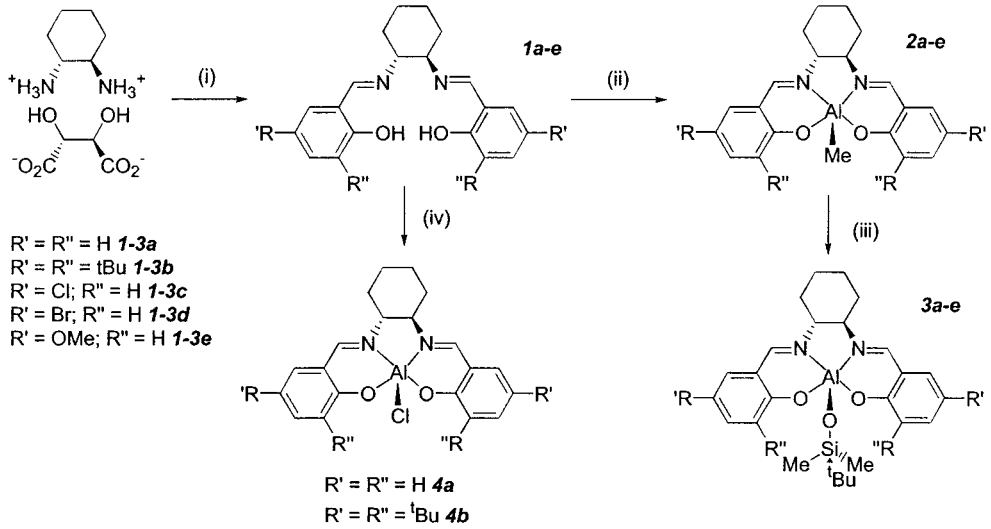


[a] Legend: (i) R′R″$C_6H_2$(OH)CHO, $K_2CO_3$, 25 °C; (ii) $AlMe_3$, toluene, reflux, 1 h; (iii) $^tBuMe_2SiOH$, toluene, 25 °C, 5 min; (iv) $AlMe_2Cl$, toluene, 25 °C, 10 h.

**Table 1**

| concn[a] | $\Lambda_M$(KCl)[b,c] | $\Lambda_M$(KCl)[d] | $\Lambda_M$(**4a**)[d] |
|---|---|---|---|
| 0.05 | 72 | 44 | |
| 0.02 | | 50 | 36 |
| 0.01 | 79 | 57 | 40 |
| 0.005 | 84 | 60 | 44 |
| 0.001 | 92 | 60 | 50 |
| 0.0005 | 98 | 60 | 50 |

[a] Concentration in mol $dm^{-3}$. [b] Molar conductivity values in $cm^2$ $\Omega^{-1}$ $M^{-1}$. [c] In $H_2O$ solvent. [d] In MeOH solvent.

**1a**)[17] reacts smoothly with alkylaluminum compounds in toluene solvent to afford both chiral organometallic and metallo-organic complexes of aluminum (Scheme 3), as reported for related Salen derivatives.[15,16] Unfortunately, as found by other workers, such organometallic Salen complexes have poor solubility in common organic solvents. Nevertheless, $^1H$ NMR spectroscopic analysis of **2a** supports a strongly shielded aluminum-bound methyl group ($\delta_H$ −1.20 ppm), while $^{27}Al$ NMR is consistent with five-coordinated aluminum in solution ($\delta_{Al}$ +52.6 ppm; $\Delta_{1/2}$ = 4.1 kHz; $CH_2Cl_2$).[17] Corresponding halide derivatives **4** are readily dissociated in donor solvents such as methanol to afford six-coordinate, bis-donor adducts with appropriate NMR (e.g. $\delta_{Al}$(**4b**) +45.9 ppm; $\Delta_{1/2}$ = 4.2 kHz; $CH_3OH$) and solution conductivity properties (Table 1). Although insoluble in water, **4a** reveals a degree of dissociation in methanol similar to that of KCl and with an expected increase in molar conductivity upon dilution. Solubility in nondonor solvents is of course improved by introducing organic functionality within the Salcyen framework, e.g. **1b** (Scheme 3), but our subsequent studies reveal the need for caution with this approach, since although solubility is improved, stereoselectivity is not necessarily increased (vide infra).

Rather than manipulating the Salcyen backbone, we reasoned that since the aluminum-bound X group functions as a sacrificial base in the PA catalytic cycle (Scheme 2), it may be substituted by a group of similar electronic character yet greater lipophilicity and hence organic solubility. For example, the *tert*-butyldimethylsiloxyl derivatives **3** are prepared by treatment of **2** with *tert*-butyldimethylsilanol (Scheme 3). Such a substitution allows far easier crystallization of **3** to high purity than for **2**, a feature with distinct impact on the catalytic chemistry (vide infra).

**Table 2. Selected Interatomic Distances (Å) for 2a**[a]

| | | | |
|---|---|---|---|
| Al(1)−O(24) | 1.806(2) | Al(1)−O(14) | 1.831(2) |
| Al(1)−C(7) | 1.968(3) | Al(1)−N(11) | 2.015(3) |
| Al(1)−N(21) | 2.038(3) | C(1)−N(11) | 1.488(4) |
| C(1)−C(6) | 1.525(4) | C(1)−C(2) | 1.536(4) |
| C(2)−N(21) | 1.469(4) | C(2)−C(3) | 1.518(4) |
| C(3)−C(4) | 1.524(4) | C(4)−C(5) | 1.528(5) |
| C(5)−C(6) | 1.538(5) | N(11)−C(12) | 1.282(4) |
| C(12)−C(13) | 1.438(5) | C(13)−C(18) | 1.408(4) |
| C(13)−C(14) | 1.413(5) | C(14)−O(14) | 1.312(4) |
| C(14)−C(15) | 1.409(5) | C(15)−C(16) | 1.383(5) |
| C(16)−C(17) | 1.390(6) | C(17)−C(18) | 1.384(5) |
| N(21)−C(22) | 1.289(4) | C(22)−C(23) | 1.437(5) |
| C(23)−C(28) | 1.405(5) | C(23)−C(24) | 1.419(5) |
| C(24)−O(24) | 1.318(4) | C(24)−C(25) | 1.408(5) |
| C(25)−C(26) | 1.392(5) | C(26)−C(27) | 1.379(6) |
| C(27)−C(28) | 1.383(5) | | |

[a] Numbers in parentheses are estimated standard deviations.

Derivatives **2a**, **3a**,**e**, and **4b** have been subjected to single-crystal X-ray analysis; crystallographic data and collection and refinement parameters for each are collected in the Supporting Information accompanying this paper. A ball-and-stick model of complex **2a** is reproduced in Figure 1 with selected bond angles and interatomic distances in Tables 2 and 3, respectively. As expected from $^{27}Al$ NMR spectroscopy, **2a** is five-coordinate with a structure which might be considered intermediate between square pyramidal and trigonal bipyramidal. Indeed, it is possible to parametrize the degree to which a five-coordinate structure approximates the former or latter geometry through a $\tau$ value where $\tau = (\beta - \alpha)/60$ and $\beta$ is the greater of the two basal angles (Figure 2).[18] For a perfect square pyramid, $\tau = 0$, and for a perfect trigonal bipyramid, $\tau = 1$.[18] For **2a**, $\beta$ = 157.24° and $\alpha$ = 136.5°, giving $\tau$ = 0.35. Complexes **3a**,**e** are structurally similar to **2a** (Figures

(17) Wei, P.; Atwood, D. A. *Polyhedron* **1999**, *18*, 641.

(18) Addison, A. W.; Rao, T. N.; Reedijk, J.; van Rijn, J.; Verscoor, G. C. *J. Chem. Soc., Dalton Trans.* **1984**, 1349.

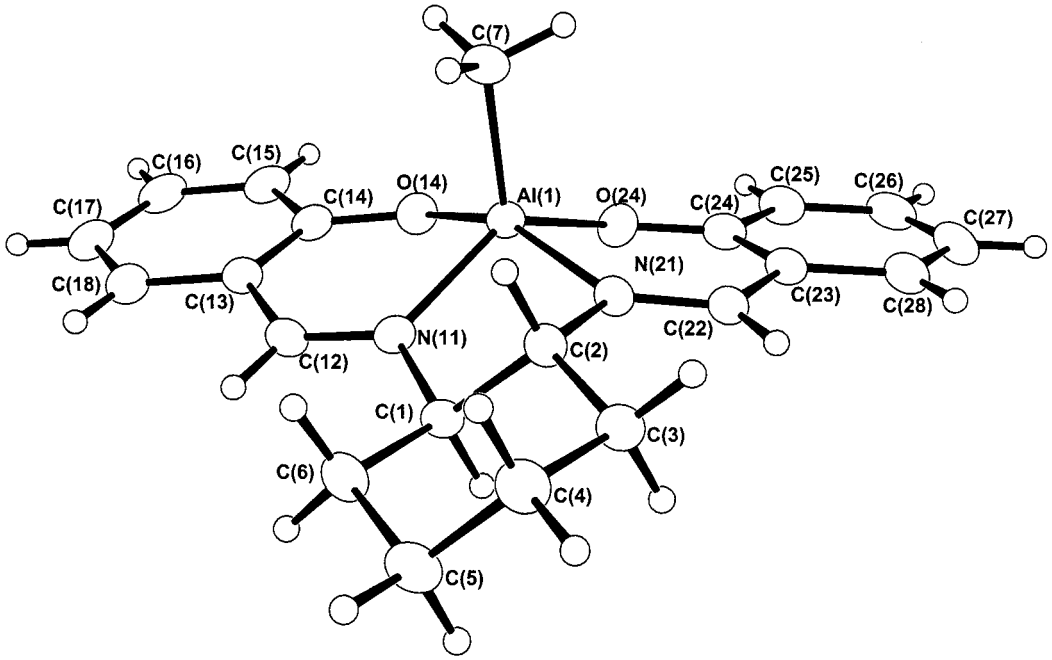


**Figure 1.** Ball and stick drawing of (*R*,*R*)-[Salcyen]AlMe (**2a**).

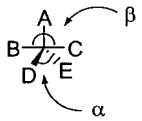


**Figure 2.** Structural parameter $\tau = (\beta - \alpha)/60$.

**Table 3. Selected Bond Angles (deg) for 2a[a]**

| | | | |
|---|---|---|---|
| O(24)−Al(1)−O(14) | 87.22(11) | O(24)−Al(1)−C(7) | 114.07(14) |
| O(14)−Al(1)−C(7) | 104.71(14) | O(24)−Al(1)−N(11) | 136.48(12) |
| O(14)−Al(1)−N(11) | 88.85(11) | C(7)−Al(1)−N(11) | 108.84(13) |
| O(24)−Al(1)−N(21) | 88.57(11) | O(14)−Al(1)−N(21) | 157.24(12) |
| C(7)−Al(1)−N(21) | 97.43(13) | N(11)−Al(1)−N(21) | 78.93(11) |
| N(11)−C(1)−C(6) | 116.1(2) | N(11)−C(1)−C(2) | 104.9(2) |
| C(6)−C(1)−C(2) | 111.4(2) | N(21)−C(2)−C(3) | 117.4(2) |
| N(21)−C(2)−C(1) | 104.2(2) | C(3)−C(2)−C(1) | 111.6(3) |
| C(2)−C(3)−C(4) | 109.2(3) | C(3)−C(4)−C(5) | 110.6(3) |
| C(4)−C(5)−C(6) | 110.8(3) | C(1)−C(6)−C(5) | 109.9(3) |
| C(12)−N(11)−C(1) | 120.1(3) | C(12)−N(11)−Al(1) | 123.6(2) |
| C(1)−N(11)−Al(1) | 116.0(2) | N(11)−C(12)−C(13) | 125.0(3) |
| C(18)−C(13)−C(14) | 120.2(3) | C(18)−C(13)−C(12) | 118.0(3) |
| C(14)−C(13)−C(12) | 121.3(3) | O(14)−C(14)−C(15) | 119.5(3) |
| O(14)−C(14)−C(13) | 122.4(3) | C(15)−C(14)−C(13) | 118.0(3) |
| C(14)−O(14)−Al(1) | 129.3(2) | C(16)−C(15)−C(14) | 120.8(3) |
| C(15)−C(16)−C(17) | 121.1(3) | C(18)−C(17)−C(16) | 119.4(3) |
| C(17)−C(18)−C(13) | 120.5(3) | C(22)−N(21)−C(2) | 122.4(3) |
| C(22)−N(21)−Al(1) | 126.6(2) | C(2)−N(21)−Al(1) | 111.1(2) |
| N(21)−C(22)−C(23) | 124.0(3) | C(28)−C(23)−C(24) | 119.9(3) |
| C(28)−C(23)−C(22) | 118.7(3) | C(24)−C(23)−C(22) | 121.3(3) |
| O(24)−C(24)−C(25) | 118.9(3) | O(24)−C(24)−C(23) | 123.1(3) |
| C(25)−C(24)−C(23) | 118.0(3) | C(24)−O(24)−Al(1) | 132.5(2) |
| C(26)−C(25)−C(24) | 120.5(4) | C(27)−C(26)−C(25) | 121.2(3) |
| C(26)−C(27)−C(28) | 119.5(3) | C(27)−C(28)−C(23) | 120.8(4) |

[a] Numbers in parentheses are the estimated standard deviations.

3 and 4 and Tables 4−7). **3a** has a $\tau$ value of $8 \times 10^{-3}$ ($\beta = 150.4°$ and $\alpha = 149.9°$), suggesting an almost perfect square plane, while **3e** has four independent molecules in the unit cell, each of which differ in the conformational properties of the siloxide function. Moreover, each molecule has a different $\tau$ value, 0.54 (150.3°), 0.47 (152.3°), 0.06 (142.5°), and 0.31 (149.8°), which correlate loosely with the Al−O−Si angle given in parentheses; the larger this latter angle, the more the overall structure tends toward trigonal bipyramidal.

**Table 4. Selected Interatomic Distances (Å) for 3a[a]**

| | | | |
|---|---|---|---|
| C(11)−N(1) | 1.297(7) | C(11)−C(12) | 1.427(7) |
| C(12)−C(17) | 1.392(7) | C(12)−C(13) | 1.427(7) |
| C(13)−O(13) | 1.317(6) | C(13)−C(14) | 1.385(7) |
| C(14)−C(15) | 1.368(8) | C(15)−C(16) | 1.398(8) |
| C(16)−C(17) | 1.361(7) | C(21)−N(2) | 1.279(7) |
| C(21)−C(22) | 1.436(7) | C(22)−C(23) | 1.390(7) |
| C(22)−C(27) | 1.407(7) | C(23)−O(23) | 1.322(6) |
| C(23)−C(24) | 1.415(7) | C(24)−C(25) | 1.373(8) |
| C(25)−C(26) | 1.380(8) | C(26)−C(27) | 1.377(7) |
| C(31)−Si(1) | 1.861(6) | C(32)−Si(1) | 1.871(6) |
| C(33)−C(35) | 1.543(7) | C(33)−C(34) | 1.548(7) |
| C(33)−C(36) | 1.553(7) | C(33)−Si(1) | 1.888(5) |
| Al(1)−O(1) | 1.720(4) | Al(1)−O(13) | 1.796(4) |
| Al(1)−O(23) | 1.805(4) | Al(1)−N(1) | 1.995(4) |
| Al(1)−N(2) | 1.997(5) | N(1)−C(1b) | 1.502(11) |
| N(1)−C(1a) | 1.511(10) | N(2)−C(2a) | 1.543(10) |
| N(2)−C(2b) | 1.563(10) | O(1)−Si(1) | 1.605(3) |
| C(1a)−C(2a) | 1.547(12) | C(1a)−C(6) | 1.574(9) |
| C(2a)−C(3) | 1.587(10) | C(3)−C(4a) | 1.568(11) |
| C(3)−C(2b) | 1.575(9) | C(3)−C(4b) | 1.616(11) |
| C(4a)−C(5a) | 1.559(13) | C(5a)−C(6) | 1.585(12) |
| C(6)−C(5b) | 1.548(11) | C(6)−C(1b) | 1.574(11) |
| C(1b)−C(2b) | 1.544(12) | C(4b)−C(5b) | 1.551(13) |

[a] Numbers in parentheses are estimated standard deviations.

Nevertheless, it is clear that complexes **3** have a significant degree of flexibility between almost perfect square planarity and up to 50% trigonal bipyramidal.

Figure 5 reveals how sterically demanding *tert*-butyl groups in the 3-position can protect the metal in **4b** from binding anything other than fairly small molecules such as water and methanol within an overall six-coordinate geometry (Tables 8 and 9). This, we also believe, has significant implications in catalysis of the phospho-aldol reaction (vide infra).

**Question 2. PA Catalysis via Aluminum−Salcyen Complexes.** Complex **2a** was found to catalyze the addition of dimethyl H-phosphonate to benzaldehyde as in Scheme 1 in a variety of solvents, including $CH_2Cl_2$, toluene, and THF, the last solvent providing greater turnover numbers within a given time period (see the Supporting Information). We subsequently examined

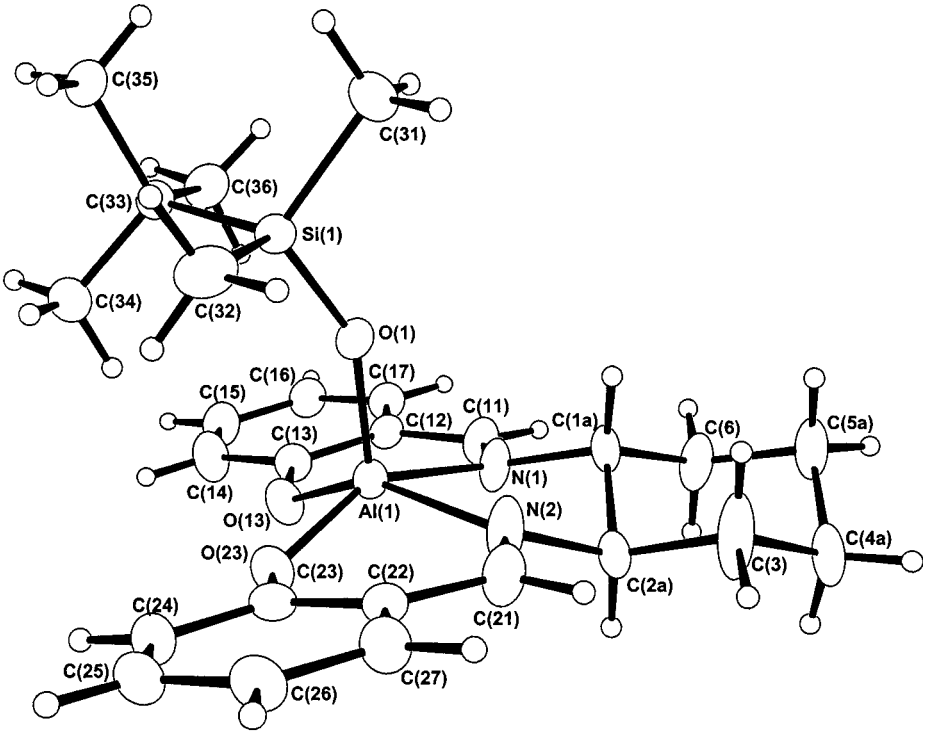


**Figure 3.** Ball and stick drawing of (*R*,*R*)-[Salcyen]AlOSiMe$_2$$^t$Bu (**3a**).

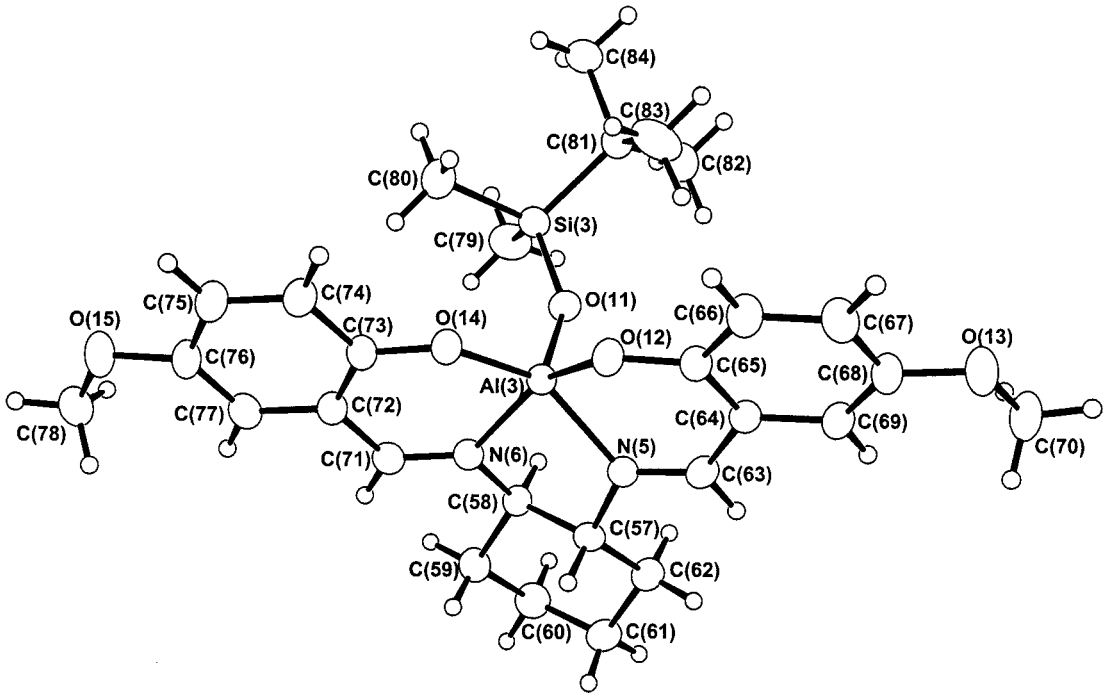


**Figure 4.** Ball and stick drawing of (*R*,*R*)-[Salcyen-OMe]AlOSiMe$_2$$^t$Bu (**3e**[2]).

the **2a**-catalyzed addition of DMHP to various substituted benzaldehydes under both aerobic and anaerobic conditions in dry THF solvent at 298 K; enantioselectivities (ee's) are collected in Table 10.

What is immediately obvious from the ee's is that the reaction appears to be tolerant to at least small amounts of water in the system. Under aerobic conditions using predried solvents and aldehydes distilled to free them from the poisoning effects of trace carboxylic acids,[19] ee's are not too dissimilar from those in which considerable precautions are taken to prevent contamination by water. However, a certain degree of care must be taken to prevent too much water in the system, since this leads to decomposition of **2a** to uncomplexed salcyen and hydrated forms of alumina. Although the former does not catalyze the phospho-aldol reaction, the latter is an effective catalyst, but obviously without engaging stereocontrol.[20] A similar explanation may be proposed for those occasions where ee's are occasionally found to be

(19) We find that trace benzoic acid in the benzaldehydes leads to formation of [salcyen]Al($O_2$CAr) complexes which, being both strongly complexed chelates and fairly insoluble in common organic solvents, are very poor catalysts and so poison the catalytic process.

(20) Villemin, D.; Ricard, M. *Tetrahedron Lett.* **1984**, *25*, 1059.

**Table 5. Selected Bond Angles (deg) for 3a[a]**

| | | | |
|---|---|---|---|
| N(1)−C(11)−C(12) | 125.0(5) | C(17)−C(12)−C(11) | 119.7(5) |
| C(17)−C(12)−C(13) | 119.5(5) | C(11)−C(12)−C(13) | 120.6(5) |
| O(13)−C(13)−C(14) | 120.4(5) | O(13)−C(13)−C(12) | 122.0(4) |
| C(14)−C(13)−C(12) | 117.6(5) | C(15)−C(14)−C(13) | 121.5(5) |
| C(14)−C(15)−C(16) | 121.1(5) | C(17)−C(16)−C(15) | 118.6(5) |
| C(16)−C(17)−C(12) | 121.7(5) | N(2)−C(21)−C(22) | 123.1(5) |
| C(23)−C(22)−C(27) | 120.1(5) | C(23)−C(22)−C(21) | 121.4(5) |
| C(27)−C(22)−C(21) | 118.4(5) | O(23)−C(23)−C(22) | 123.3(5) |
| O(23)−C(23)−C(24) | 118.8(5) | C(22)−C(23)−C(24) | 117.9(5) |
| C(25)−C(24)−C(23) | 121.0(5) | C(24)−C(25)−C(26) | 121.0(5) |
| C(27)−C(26)−C(25) | 119.1(5) | C(26)−C(27)−C(22) | 120.9(5) |
| C(35)−C(33)−C(34) | 109.1(4) | C(35)−C(33)−C(36) | 108.0(4) |
| C(34)−C(33)−C(36) | 108.0(5) | C(35)−C(33)−Si(1) | 110.9(4) |
| C(34)−C(33)−Si(1) | 109.8(4) | C(36)−C(33)−Si(1) | 110.9(3) |
| O(1)−Al(1)−O(13) | 109.0(2) | O(1)−Al(1)−O(23) | 107.9(2) |
| O(13)−Al(1)−O(23) | 88.6(2) | O(1)−Al(1)−N(1) | 100.7(2) |
| O(13)−Al(1)−N(1) | 89.2(2) | O(23)−Al(1)−N(1) | 150.4(2) |
| O(1)−Al(1)−N(2) | 100.3(2) | O(13)−Al(1)−N(2) | 149.9(2) |
| O(23)−Al(1)−N(2) | 88.6(2) | N(1)−Al(1)−N(2) | 78.9(2) |
| C(11)−N(1)−C(1b) | 118.9(5) | C(11)−N(1)−C(1a) | 120.9(5) |
| C(1b)−N(1)−C(1a) | 32.1(5) | C(11)−N(1)−Al(1) | 124.4(4) |
| C(1b)−N(1)−Al(1) | 115.1(5) | C(1a)−N(1)−Al(1) | 111.5(4) |
| C(21)−N(2)−C(2a) | 117.2(6) | C(21)−N(2)−C(2b) | 119.5(5) |
| C(2a)−N(2)−C(2b) | 37.2(5) | C(21)−N(2)−Al(1) | 126.1(4) |
| C(2a)−N(2)−Al(1) | 114.9(4) | C(2b)−N(2)−Al(1) | 110.1(4) |
| Si(1)−O(1)−Al(1) | 148.9(2) | C(13)−O(13)−Al(1) | 129.7(3) |
| C(23)−O(23)−Al(1) | 128.5(3) | O(1)−Si(1)−C(31) | 108.2(2) |
| O(1)−Si(1)−C(32) | 112.0(2) | C(31)−Si(1)−C(32) | 106.9(3) |
| O(1)−Si(1)−C(33) | 110.3(2) | C(31)−Si(1)−C(33) | 109.9(3) |
| C(32)−Si(1)−C(33) | 109.5(3) | N(1)−C(1a)−C(2a) | 100.9(7) |
| N(1)−C(1a)−C(6) | 112.4(7) | C(2a)−C(1a)−C(6) | 106.6(7) |
| N(2)−C(2a)−C(1a) | 98.5(7) | N(2)−C(2a)−C(3) | 110.3(7) |

[a] Numbers in parentheses are the estimated standard deviations.

**Table 6. Selected Interatomic Distances (Å) for 3e[a]**

| | | | |
|---|---|---|---|
| Molecule **3e[1]** | | | |
| Al(2)−O(6) | 1.724(2) | Al(2)−O(9) | 1.793(2) |
| Al(2)−O(7) | 1.810(2) | Al(2)−N(4) | 2.012(2) |
| Al(2)−N(3) | 2.020(2) | Si(2)−O(6) | 1.603(2) |
| Si(2)−C(52) | 1.869(4) | Si(2)−C(51) | 1.870(3) |
| Si(2)−C(53) | 1.893(3) | O(7)−C(37) | 1.327(3) |
| O(8)−C(40) | 1.385(3) | O(8)−C(42) | 1.433(4) |
| O(9)−C(45) | 1.333(3) | O(10)−C(48) | 1.383(4) |
| O(10)−C(50) | 1.418(5) | N(3)−C(43) | 1.290(3) |
| N(3)−C(29) | 1.474(3) | N(4)−C(35) | 1.288(3) |
| N(4)−C(30) | 1.482(3) | C(29)−C(34) | 1.523(4) |
| Molecule **3e[2]** | | | |
| Al(3)−O(11) | 1.724(2) | Al(3)−O(14) | 1.794(2) |
| Al(3)−O(12) | 1.814(2) | Al(3)−N(5) | 2.017(2) |
| Al(3)−N(6) | 2.026(2) | Si(3)−O(11) | 1.613(2) |
| Si(3)−C(79) | 1.857(4) | Si(3)−C(80) | 1.877(3) |
| Si(3)−C(81) | 1.893(3) | O(12)−C(65) | 1.325(3) |
| O(13)−C(68) | 1.380(3) | O(13)−C(70) | 1.429(4) |
| O(14)−C(73) | 1.334(3) | O(15)−C(76) | 1.391(3) |
| O(15)−C(78) | 1.424(4) | N(5)−C(63) | 1.287(3) |
| N(5)−C(57) | 1.481(3) | N(6)−C(71) | 1.295(3) |

[a] Numbers in parentheses are estimated standard deviations.

dependent upon the specific synthetic history of **2a**; adventitious exposure to moisture during the preparation of **2a** results in formation of contaminating aluminas, thus leading to effective catalysis but with overall lowered ee's. Unfortunately, it is not a trivial matter to purify **2a** by recrystallization, due to the latter's insolubility in common organic solvents. For this reason, we have shifted our attention to Al−OSiMe$_2$tBu derivatives (Scheme 3), which we find to be far more soluble and hence far easier to purify and which do not afford significantly different ee's in reaction with substituted benzaldehydes (Table 11).

It is obviously vital to ensure that the product α-hydroxyphosphonate esters are configurationally stable in the presence of (i) metallo-organic Salcyen compounds and (ii) quinine chiral solvating agents. Our experiments (see Experimental Section) reveal in both cases that such configurational integrity is retained, at least during the lifetime of our experiments.

**Table 7. Selected Bond Angles (deg) for 3e[a]**

| | | | |
|---|---|---|---|
| Molecule **3e[1]** | | | |
| O(6)−Al(2)−O(7) | 103.92(10) | O(9)−Al(2)−O(7) | 89.43(9) |
| O(6)−Al(2)−N(4) | 108.40(9) | O(9)−Al(2)−N(4) | 134.34(9) |
| O(7)−Al(2)−N(4) | 89.85(9) | O(6)−Al(2)−N(3) | 92.59(10) |
| O(9)−Al(2)−N(3) | 88.71(10) | O(7)−Al(2)−N(3) | 162.41(9) |
| N(4)−Al(2)−N(3) | 79.05(9) | O(6)−Si(2)−C(52) | 109.9(2) |
| O(6)−Si(2)−C(51) | 109.5(2) | C(52)−Si(2)−C(51) | 109.1(2) |
| O(6)−Si(2)−C(53) | 109.82(12) | C(52)−Si(2)−C(53) | 109.7(2) |
| C(51)−Si(2)−C(53) | 108.9(2) | Si(2)−O(6)−Al(2) | 152.27(14) |
| C(37)−O(7)−Al(2) | 130.9(2) | C(40)−O(8)−C(42) | 116.2(2) |
| C(45)−O(9)−Al(2) | 130.1(2) | C(48)−O(10)−C(50) | 116.1(3) |
| C(43)−N(3)−C(29) | 121.6(2) | C(43)−N(3)−Al(2) | 126.4(2) |
| C(29)−N(3)−Al(2) | 111.8(2) | C(35)−N(4)−C(30) | 119.2(2) |
| C(35)−N(4)−Al(2) | 124.6(2) | C(30)−N(4)−Al(2) | 116.1(2) |
| N(3)−C(29)−C(34) | 117.5(2) | N(3)−C(29)−C(30) | 104.5(2) |
| C(34)−C(29)−C(30) | 111.8(2) | N(4)−C(30)−C(31) | 116.4(2) |
| Molecule **3e[2]** | | | |
| O(11)−Al(3)−O(14) | 109.99(9) | O(11)−Al(3)−O(12) | 107.88(9) |
| O(14)−Al(3)−O(12) | 88.34(9) | O(11)−Al(3)−N(5) | 101.72(9) |
| O(14)−Al(3)−N(5) | 147.57(9) | O(12)−Al(3)−N(5) | 88.33(9) |
| O(11)−Al(3)−N(6) | 100.08(9) | O(14)−Al(3)−N(6) | 88.82(9) |
| O(12)−Al(3)−N(6) | 151.12(9) | N(5)−Al(3)−N(6) | 78.92(9) |
| O(11)−Si(3)−C(79) | 108.93(13) | O(11)−Si(3)−C(80) | 112.16(12) |
| C(79)−Si(3)−C(80) | 107.5(2) | O(11)−Si(3)−C(81) | 109.25(11) |
| C(79)−Si(3)−C(81) | 111.7(2) | C(80)−Si(3)−C(81) | 107.39(14) |
| Si(3)−O(11)−Al(3) | 142.52(12) | C(65)−O(12)−Al(3) | 129.1(2) |
| C(68)−O(13)−C(70) | 116.2(2) | C(73)−O(14)−Al(3) | 133.4(2) |
| C(76)−O(15)−C(78) | 116.5(2) | C(63)−N(5)−C(57) | 119.6(2) |
| C(63)−N(5)−Al(3) | 123.6(2) | C(57)−N(5)−Al(3) | 116.8(2) |
| C(71)−N(6)−C(58) | 120.8(2) | C(71)−N(6)−Al(3) | 126.8(2) |
| C(58)−N(6)−Al(3) | 112.2(2) | N(5)−C(57)−C(58) | 106.8(2) |

[a] Numbers in parentheses are the estimated standard deviations.

**Table 8. Selected Interatomic Distances (Å) for 4b**

| | | | |
|---|---|---|---|
| Al(1)−O(23) | 1.7999(12) | Al(1)−O(13) | 1.8002(13) |
| Al(1)−O(9) | 1.9632(14) | Al(1)−O(7) | 1.9749(14) |
| Al(1)−N(1) | 1.9952(14) | Al(1)−N(2) | 1.996(2) |
| O(7)−C(8) | 1.411(3) | O(9)−C(10) | 1.384(3) |
| C(1)−N(1) | 1.478(2) | C(1)−C(6) | 1.524(2) |
| C(1)−C(2) | 1.534(2) | C(2)−N(2) | 1.478(2) |
| C(2)−C(3) | 1.529(2) | C(3)−C(4) | 1.534(3) |
| C(4)−C(5) | 1.515(3) | C(5)−C(6) | 1.531(3) |
| N(1)−C(11) | 1.290(2) | N(2)−C(21) | 1.280(2) |
| O(1s)−C(1s) | 1.366(6) | O(2s)−C(2s) | 1.099(9) |
| C(2s)−O(3s) | 1.148(12) | | |

[a] Numbers in parentheses are estimated standard deviations.

**Table 9. Selected Bond Angles (deg) for 4b[a]**

| | | | |
|---|---|---|---|
| O(23)−Al(1)−O(13) | 96.43(6) | O(23)−Al(1)−O(9) | 92.40(6) |
| O(13)−Al(1)−O(9) | 91.65(6) | O(23)−Al(1)−O(7) | 91.70(6) |
| O(13)−Al(1)−O(7) | 91.72(6) | O(9)−Al(1)−O(7) | 174.37(6) |
| O(23)−Al(1)−N(1) | 172.03(6) | O(13)−Al(1)−N(1) | 91.53(6) |
| O(9)−Al(1)−N(1) | 86.85(6) | O(7)−Al(1)−N(1) | 88.55(6) |
| O(23)−Al(1)−N(2) | 91.16(6) | O(13)−Al(1)−N(2) | 172.39(6) |
| O(9)−Al(1)−N(2) | 88.53(6) | O(7)−Al(1)−N(2) | 87.54(6) |
| N(1)−Al(1)−N(2) | 80.89(6) | | |
| C(8)−O(7)−Al(1) | 126.8(2) | C(10)−O(9)−Al(1) | 129.32(14) |
| N(1)−C(1)−C(6) | 117.23(14) | N(1)−C(1)−C(2) | 105.80(12) |
| C(6)−C(1)−C(2) | 111.27(14) | N(2)−C(2)−C(3) | 116.74(14) |
| N(2)−C(2)−C(1) | 105.74(12) | C(3)−C(2)−C(1) | 110.70(14) |
| C(2)−C(3)−C(4) | 109.4(2) | C(5)−C(4)−C(3) | 111.8(2) |
| C(4)−C(5)−C(6) | 111.3(2) | C(1)−C(6)−C(5) | 109.6(2) |
| C(11)−N(1)−C(1) | 121.56(13) | C(11)−N(1)−Al(1) | 124.09(11) |
| C(1)−N(1)−Al(1) | 114.30(10) | | |

[a] Numbers in parentheses are the estimated standard deviations.

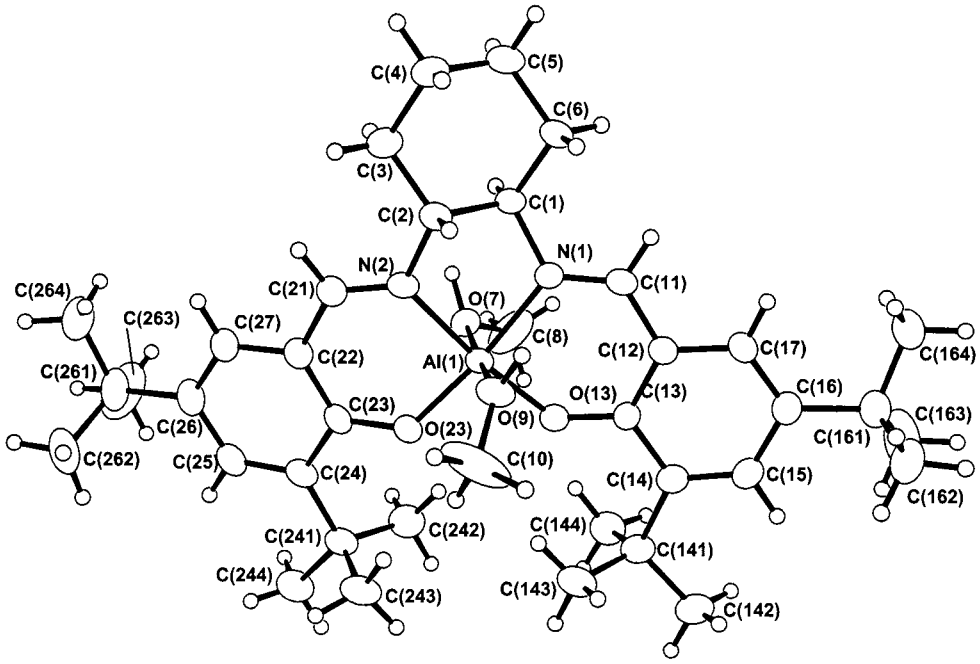


**Figure 5.** Ball and stick drawing of {(*R*,*R*)-[Salcyen]Al(MeOH)$_2$}Cl (**4b**).

**Table 10. Enantioselectivities in the Reactions between DMHP (1 mmol) and ArCHO (1 mmol) Catalyzed by 2a at 298 K in THF Solvent**[a]

| aldehyde | entry | ee (%)[b] | ee (%)[c] | ee (%)[d] |
|---|---|---|---|---|
| $C_6H_5CHO$ | 1 | 37 (*R*) | 41 (*R*) | 45 (*R*) |
| 4-$BrC_6H_4CHO$ | 2 | 27 (*R*) | 24 (*R*) | 21 (*R*) |
| 4-$MeC_6H_4CHO$ | 3 | 44 (*R*) | 49 (*R*) | 46 (*R*) |
| 4-$MeOC_6H_4CHO$ | 4 | 39 (*R*) | 46 (*R*) | 49 (*R*) |
| 4-$O_2NC_6H_4CHO$ | 5 | 15 (*R*) | 10 (*R*) | |
| 4-$ClC_6H_4CHO$ | 6 | 30 (*R*) | 19 (*R*) | |
| 2-$ClC_6H_4CHO$ | 7 | 12 (*R*) | 12 (*R*) | |
| 2-$MeC_6H_4CHO$ | 8 | 25 (*R*) | 20 (*R*) | |
| 2-$MeOC_6H_4CHO$ | 9 | 20 (*R*) | 27 (*R*) | |

[a] All reactions were analyzed after 48 h, each reaction having proceeded to completion. Catalyst loading was 5 mol %. [b] Reactions performed under dry inert-atmosphere conditions. [c] Reactions performed under aerobic conditions. ee's were determined by $^{31}P\{^1H\}$ NMR using quinine as a chiral solvating agent. Absolute configurations are given in parentheses. [d] Using **3a** as catalyst.

Enantioselectivities have been determined by $^{31}P\{^1H\}$ NMR spectroscopy using quinine as a chiral solvating agent,[21] a technique and reagent already used with considerable success for α-hydroxyphosphonate systems.[22] Absolute configurations are envisaged to be all *R* on the basis that the optical rotation $[\alpha]^D$ of $(MeO)_2P(O)CH(OH)C_6H_4Me$-4 (39% ee) was found to be +17.1° ($c$ = 1; $CHCl_3$). Given that the vast majority of *R*-configuration α-hydroxyphosphonate esters derived from aromatic benzaldehydes possess *positive* optical rotations[23] and that, in each case, we observe the same stereoisomer dominating by $^{31}P$ NMR (unless noted otherwise), we envisage the same sense of stereocontrol in this closely related family of compounds in our system.

**Question 3. Structure−Activity Analysis of Asymmetric Phospho-Aldol Catalysis.** It is immediately obvious from the data in Table 10 that enantioselectivity is dependent upon the nature of the aldehyde. Consideration of entries 1−6 reveals that ee's decrease as the *para* substituent on the benzaldehyde become more electron withdrawing, a trend made more obvious through a plot (Supporting Information) of $\log(ee_{Ar}/ee_{Ph})$ versus the Hammett $\sigma_p$ parameters of the *para* substituents.[24] The negative gradient returns a $\rho$ value of −0.42, similar to that reported by Shibuya et al. in their lanthanide phospho-aldol system. Such a correlation is consistent with binding of the carbonyl to a Lewis acidic center being important in the enantiodetermining step.[6i] However, we recognize also that the $\rho$ value observed in our aluminum system is significantly smaller than that observed in Shibuya's lanthanum binaphthol system ($\rho = -1.3$), suggesting a weaker overall electronic influence consistent with the lower electropositivity of aluminum over lanthanum.

Benzaldehyde substitution in the *ortho* position (entries 7−9; Table 11) leads consistently to lower ee's than for *para* substitution; presumably steric factors are likely to play a more significant role here (vide infra).

The same data have been recorded also in $d_8$-toluene solvent, where it is found that there are some differences in ee compared to those in THF solvent. It is clear, though, that there is an electronic influence upon ee exerted by the aldehyde substrate. We have examined whether there might also be an electronic influence upon ee caused by substitution at the R′ position of the catalyst ligand framework (Scheme 3). We recognize that such substitution is six bonds distant from the catalyst metal center and thus may not necessarily have

(21) See for example: Parker, D. *Chem. Rev.* **1991**, *91*, 1441. Hulst, R.; Kellogg, R. M.; Feringa, B. L. *Recl. Trav. Chim. Pays-Bas* **1995**, *115*, 114 and references therein.

(22) Zymanczyk-Duda, E.; Skwarczynski, M.; Lejczak, B.; Kafarski, P. *Tetrahedron: Asymmetry* **1996**, *7*, 1277.

(23) Gajda, T *Tetrahedron: Asymmetry* **1994**, *5*, 1965; Smaardijk, A. A.; Noorda, S.; Van Bolhuis F.; Wynberg, H. *Tetrahedron Lett.* **1985**, *26*, 493. Meier, C.; Laux, W. H. G. *Tetrahedron: Asymmetry* **1995**, *6*, 1089.

(24) March, J. *Advanced Organic Chemistry*, 3rd ed.; Wiley: New York, 1985; Chapter 9. We have chosen to represent the relationship of $\log(ee_{Ar}/ee_{Ph})$ rather than $\log k_{R/S}$, since in a kinetically controlled reaction such as this, the relative enantiomeric composition of the products will be proportional to their rates of formation. Moreover, comparison is easier with the analogous data reported by Shibuya et al.[6i]

**Scheme 4**

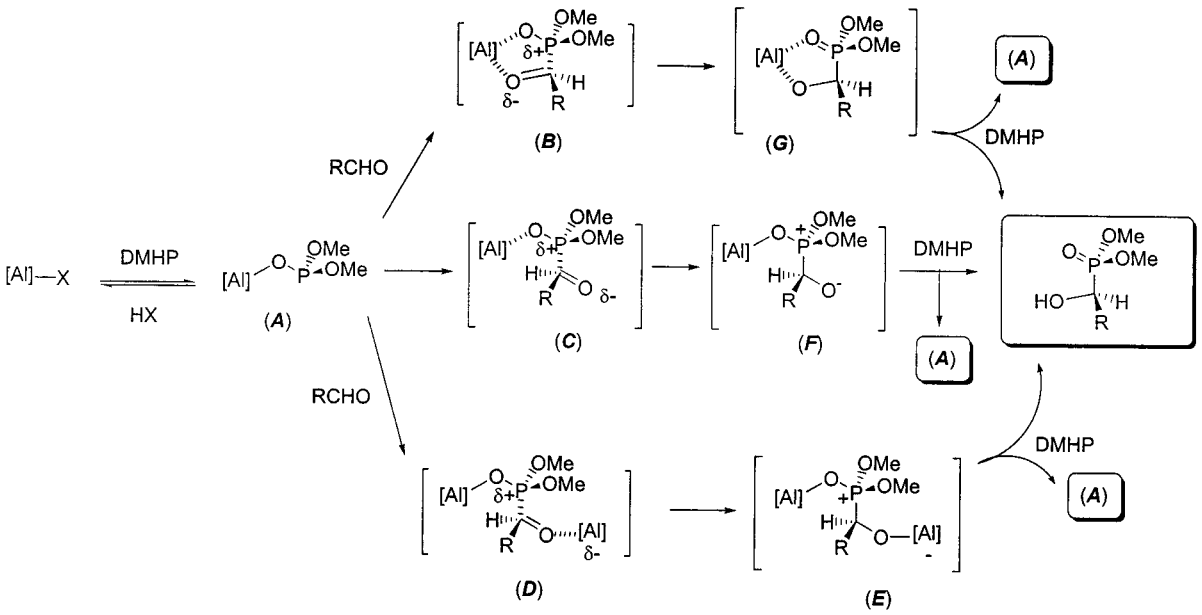




a profound effect. Indeed, the standard ee deviations across R′ = H, Cl, Br, and OMe rather suggest this to be the case. Although there is some difference in absolute selectivities between THF and toluene solvent, it is still clear that greater selectivities are returned for the less activated carbonyls, again consistent with the idea that higher ee's result from activation of the carbonyl by binding to a metal center (Supporting Information).

In addition to enantioselectivity being dependent upon the nature of benzaldehyde substitution, reaction rates are also influenced significantly by this aldehyde substitution and by the nature of substitution in the ligand framework of the catalyst. Thus, when DMHP is reacted with ArCHO in the presence of **3a** (2 mol %), the number of catalytic turnovers achieved after 150 min in $d_8$-toluene has been determined by $^{31}P\{^1H\}$ NMR spectroscopy and tabulated for both a range of substituted benzaldehydes and for substituted salcyen complexes **3a**−**e** (Supporting Information). It is reasonably clear that carbonyl substitution has a more profound effect on both reaction rate and ee than does the substitution pattern in the catalyst ligand backbone. The more electron withdrawing, and hence carbonyl activating, benzaldehyde substituents result in more rapid phospho-aldol reactions.

We have performed a more rigorous kinetic analysis of the addition of DMHP to substituted benzaldehydes, catalyzed by complexes **3a**−**e**, with a view to probing mechanistic features of the reaction in more detail. We worked on the basis that, in the absence of complicating features, the phospho-aldol addition should essentially be a second-order process (Scheme 1) and, consequently, one has two options when planning kinetic experiments: (i) maintaining second-order kinetics by arranging for [DMHP] = [ArCHO] or (ii) working under pseudo-first-order conditions where one reagent is in large excess over the other. In practice, we found the latter led to solubility difficulties which compromised quantitative analysis to an unacceptable degree. Consequently, our initial kinetic studies were performed according to second-order conditions under protocol (i). Under these conditions, ($d_8$-toluene, 300 K) the standard second-order equation, $x/([A_0] - x)[A_0] = k_2t$, where $k_2$ is the second-order rate constant, $x$ is the degree of reaction, and $[A_0]$ denotes the initial concentrations of both DMHP and aldehyde, does not produce a satisfactory linear relationship. Instead, excellent agreement is found against a second-order polynomial of the type $x/([A_0] - x)[A_0] = k_2t + k_{2'}t^2$, where $k_2$ and $k_{2'}$ are constants (Supporting Information), suggesting somewhat more complex behavior than would be expected from a simple second-order mechanism. Reaction is faster with more electron-withdrawing substituents on the aldehyde substrate, as expected, although whether 2- or 4-substitution results in a faster reaction seems to depend on the metal complex used. Addition of excess water (2 mol equiv) results in considerable loss of catalytic activity, whereas addition of molecular sieve prior to initiating catalysis results in increased reactivity. Addition of $^t$BuMe$_2$SiOH (5 mol %) also results in attenuation of activity (vide infra).

## Discussion

A generally accepted mechanism of the phospho-aldol reaction is illustrated in Scheme 4. The initial step involves deprotonation of DMHP by the polar $Al^{\delta+}-X^{\delta-}$ bond to afford an intermediate metallo-phosphite (**A**). Even though it has not proved possible to observe directly the presence of **A**, there is considerable precedent for such compounds.[25] We envisage **A** to be highly reactive in the presence of electrophiles such as aldehydes, and not surprisingly, we were unable to detect its presence directly when reaction was followed by $^{31}P$ NMR spectroscopy at 25 °C. Moreover, allowing the reaction to proceed partially followed by cooling to low temperature and analysis via $^{31}P$ NMR also failed to provide direct evidence for the presence of **A**. Nevertheless, it is well-known that trivalent phosphito analogues of **A** such as silyl phosphite esters react smoothly and

(25) See for example: Issleib, K.; Walther, B. *Angew. Chem.* **1967**, *6*, 88.

quantitatively with aldehydes to afford α-siloxyphosphonate esters.[26] Indeed, this variant is a close relative of the phospho-aldol reaction called the phospho-Mukaiyama aldol reaction, and use of chiral silyl phosphite esters allows control of stereochemistry at the newly created α-carbon atom of the product phosphonate ester.[27]

Consequently, it is clear that complexes **2a**−**e** and **3a**−**e** are not strictly catalysts but, more precisely, catalyst precursors where the X function must first be lost as HX in reaction with DMHP. Obviously this results in an equilibrium (Scheme 4), the position of which we would expect to depend on the relative p$K_a$'s of DMHP and HX. The p$K_a$ of DMHP has not been measured but has been calculated to be ca. 14 on the basis of theoretical data.[28] Consequently, the lower the p$K_a$ of HX, the more the pre-equilibrium in Scheme 4 will lie toward [Al]−X and the lower the concentration of **A** will be and, thus, reaction rates should be lowered as a consequence. Indeed, we find that halide complexes **4a**,**b** are far poorer catalyst precursors than either methyl or siloxide derivatives **2** or **3**. We might expect also that addition of $^t$BuMe$_2$SiOH to a phospho-aldol reaction mixture catalyzed by complexes **3** should lead to catalyst inhibition as the pre-equilibrium is shifted to the left-hand side. Although it is clear that the reaction is tolerant to small quantities of water, it is equally clear that too much water leads to attenuation of catalytic activity. We suppose that this is a result of decomposition of the catalyst to aluminum hydroxide, which precipitates from solution. Even though basic alumina is known to be an effective phospho-aldol catalyst, addition of water suppresses catalytic activity. Further support for the deleterious effect of water comes from the fact that pretreating a phospho-aldol mixture of DMHP, PhCHO in THF with 4 Å molecular sieves prior to introduction of catalyst results in increased catalytic activity.

Reaction of **A** with aldehyde is the important step where a new stereocenter is created. Three possibilities come to mind for this stereodetermining step: (i) monometallic P−C bond formation via a closed transition state (**B**), (ii) monometallic P−C bond formation via an open transition state (**C**), and (iii) bimetallic P−C bond formation via an open transition state (**D**) (Scheme 4).

We envisage that all three P−C bond forming steps may operate in parallel, resulting in an overall enantioselectivity ee which is a composite of three individual terms for each of the individual processes, ee = ee$_\mathbf{B}$ + ee$_\mathbf{C}$ + ee$_\mathbf{D}$. It is further envisaged that since transition states **B** and **D** contain *both* phosphorus and carbonyl substrate within a chiral environment, these are the processes which should result in the largest ee's. This must remain, however, a proposal only in the absence of corroborative evidence. In each of these three reaction scenarios, an intermediate metal alkoxide is produced (**E**−**G**), which undergoes proton transfer with DMHP to afford decomplexed α-hydroxyphosphonate ester and regenerate intermediate **A**. Although we do not observe **E**−**G** directly, there is significant precedent for metal alkoxides as phospho-aldol catalysts. For instance, we have demonstrated that Li$O^t$Bu is an excellent catalyst precursor for the addition of DMHP to benaldehyde and, more significantly, we note that **3a**−**e** are excellent and enantioselective catalyst precursors.

Our kinetic analyses reveal that the reaction does not follow perfect second-order behavior but possesses an additional term, $x/([A_0] - x)[A_0] = k_2t + k_{2'}t^2$, which suggests perhaps that the reaction is slightly faster than expected on the basis of standard second-order behavior. An explanation for this is not immediately obvious, although one possibility is that catalysis requires three steps: (1) initiation, (2) initial [P−C] bond formation via intermediate **A**, and (3) subsequent catalytic turnover via intermediates such as **E**−**G**. The reaction rate is likely to be dependent upon varying concentrations of **A** and **E**−**G**. One possibility could be that reaction is somewhat slower than expected in the initial stages due to the need to convert our catalyst precursor to **A** in Scheme 4. However, it is also clear that in a minority of cases, such as the reactions of DMHP with 4-Br$C_6H_4$-CHO and 2-Br$C_6H_4$CHO catalyzed by **3e**, attenuation of catalytic activity with time is observed. Again, precise explanations are uncertain, but gradual binding of catalytic metal complex byproduct phosphonate ester may be one possibility, although it is unclear why only these particular esters should be so affected.

Our working assumption then, based on our own work and previous work of Shibuya and Shibasaki,[6] is that intimate contact between both phosphorus and carbonyl components and the chiral catalytic center is necessary in order to achieve the highest ee's. What is immediately obvious from the crystal structures of the catalytic precursors **2a** and **3a**,**e** in Figures 1, 3, and 4 is that the source of chirality is quite distant from the active metal center and at least four to five bonds distant from the newly created stereocenter. By what mechanism can stereodifferentiating information be passed from the backbone cyclohexyl function to the active phosphorus and carbon centers in transition states **B**−**D**? Our working hypothesis focuses on the crucial intermediate **A**, which we presume will have a structure similar to **3a**,**e,** given the isoelectronic relationship between OP(OMe)$_2$ and OSiMe$_2$tBu. Significantly, we noted in our structural discussions above that there are four independent molecules of **3e** in the unit cell, each with a different $\tau$ value, 0.54 (150.3°), 0.47 (152.3°), 0.06 (142.5°), and 0.31 (149.8°), which correlates loosely with the Al−O−Si angle (in parentheses): the larger the angle, the more the overall structure tends toward trigonal bipyramidal. We envisage that as carbonyl approaches phosphito complex **A** via the closed transition state **B**, there is considerable potential for distortion toward either a square pyramid or trigonal bipyramid, leading to transition states with different degrees of chiral ligand twisting (Figure 6). We envisage that the more twisted structure, (a), will afford a greater degree of asymmetry in the immediate P−C bond forming transition state than will (b). Even though it is known for Salcyen type ligands to occupy twisted or facial coordination environments in metal complexes,[29] it is

(26) Evans, D. A.; Hurst, K. M.; Takacs, J. M. *J. Am. Chem. Soc.* **1978**, *100*, 3467.
(27) Sum, V.; Baird, C. A.; Kee, T. P.; Thornton-Pett, M. *J. Chem. Soc., Perkin Trans. 1* **1994**, 3183.
(28) Guthrie, J. P. *Can. J. Chem.* **1979**, *57*, 236.
(29) See for example: Corden, J. P.; Errington, W.; Moore, P.; Wallbridge, M. G. H. *Chem. Commun.* **1999**, 323.

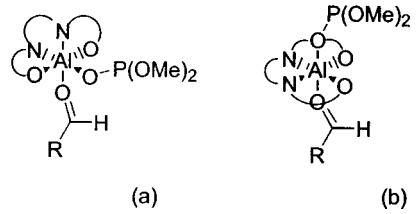


**Figure 6.**

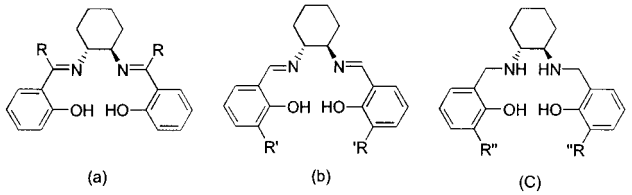


**Figure 7.**

far more common for them to display meridional geometries.[13−17]

Consequently, we envisage that increasing the degree of flexibility within the chiral ligand framework to better achieve a twisted structure will be advantageous, since it is clear that the ee increases with increasing electron richness of the benzaldehyde substrate, consistent with binding of this substrate to the metal center resulting in increased selectivity.[6i] However, one must exercise some care in choosing an appropriate method to introduce flexibility. Three mechanisms immediately suggest themselves (Figure 7). Since we experienced synthetic difficulties in preparing the corresponding aluminum complexes **7**(a), we have focused our attention on derivatives (b) and (c). Substitution of ligand hydrogen atoms by the sterically demanding function R′ could lead to steric pressure which might help in ligand twisting at the metal. However, if twisting does not occur, then we might expect both slower reaction and poorer ee's, since sterically demanding R′ groups could prevent approach and binding of carbonyl to the metal. Revealingly, we find that **2b** acts as a catalyst precursor in the phospho-aldol reaction but reaction is slower than with **2a** and results in both significantly lower ee's (<13%) and, in most cases, opposite absolute configuration. It is well-known that ligand **1b** is capable of binding to a metal in a meridional manner, and it seems reasonable from the structural work of others and ours here on **4b** (Figure 5) that although small molecules such as methanol and water can bind quite well within the cavity created by **1b**, larger molecules such as aldehydes might be expected to experience steric problems. We envisage, therefore, that **2b** catalyzes principally via the **A**−**C**−**F** pathway in Scheme 4 and that this pathway leads to lower stereoselectivities, as expected, and favors, to at least some extent, *S* absolute configurations of the product phosphonate.

Our most recent, as yet unpublished, work focuses therefore upon the reduced Salcyan ligand motif of Figure 7c, where we anticipate that increased flexibility engendered by reduction of C=N to CH−NH may allow sterically discriminating substituents R″ to encourage a twisted facial coordination geometry at the metal center (Figure 6). Indeed, our preliminary studies on the new hydroxo-bridged dimer {(*R*,*R*)-[$^t$Bu-Salcyan]Al-($\mu$-OH)}$_2$ suggest a considerable difference compared to Salcyen systems.[30]



## Experimental Section

**General Information.** Where appropriate, all manipulations were carried out under aerobic conditions unless stated otherwise. Inert-atmosphere operations were performed under dry nitrogen using standard Schlenk line and cannula techniques. Solvents were predried over sodium wire or calcium chloride prior to being heated under reflux and subsequently being distilled from the appropriate drying agent (in parentheses): pentane ($LiAlH_4$), THF (sodium benzophenone ketyl), toluene (sodium metal), and dichloromethane (calcium hydride). All solvents were deoxygenated immediately prior to use. NMR spectra were recorded at 298 K, unless stated otherwise, on JEOL FX90 (operating frequency for $^{31}$P of 36.2 MHz), JEOL FX100 (operating frequencies for $^1$H and $^{31}$P of 99.5 and 40.3 MHz, respectively), Bruker AM400 ($^1$H at 400.1 MHz and $^{13}$C at 100.6 MHz), and Bruker ARX250 instruments ($^1$H at 250.1 MHz, $^{31}$P at 101.6 MHz, and $^{13}$C at 62.9 MHz). Chemical shifts are reported in ppm and referenced to either residual proton resonances in the deuterated solvent used or tetramethylsilane (as 0 ppm), while $^{31}$P shifts are referenced to external 85% $H_3PO_4$ unless stated otherwise. All couplings are quoted in hertz (Hz). Deuterated solvents were dried by flash filtration on a short column (2−3 cm) of basic Brockmann grade I alumina and were deoxygenated before use. The Microanalytical Laboratory of the School of Chemistry at Leeds performed elemental analyses. Mass spectra were collected by the Leeds University Mass Spectrometric Service on a VG Autospec instrument operating in the electron impact (70 eV) mode unless noted otherwise. The isotopic mass error ($\sigma$) on all high-resolution mass peaks reported is within 10 ppm. Infrared spectra were recorded as KBr disks, thin films, or Nujol mulls using a Perkin-Elmer 257 grating spectrophotometer (4000−600 cm$^{-1}$); all absorptions are quoted in wavenumbers (cm$^{-1}$). Optical rotations were recorded on an Optical Activity AA 10 polarimeter operating at 589.44 nm (sodium D line). TLC was performed on plates precoated to a thickness of 0.25 mm with CAMLAB-Fertigplatten SIL G-25 $UV_{254}$ and visualized by ultraviolet light, aqueous potassium permanganate solution, or iodine vapor. Silica gel for all column chromatography was commercial Merck grade 9385 (230−400 mesh) and used as received. The compounds (±)-*trans*-1,2-diaminocyclohexane, phosphorus trichloride, *l*-(+)-tartaric acid, trimethylaluminum, chlorodimethylaluminum, and all carbonyl compounds were purchased from commercial sources and used as received. Triethylamine and *N*-methylmorpholine were predried by filtration on a short column (2−3 cm) of basic Brockmann grade I alumina immediately prior to use. (*R*,*R*)-(+)-1,2-Diaminocyclohexane-L-tartrate, (*R*,*R*)-Salcyen, 3,5-di-*tert*-butylsalicylaldehyde, and (*R*,*R*)-[$^t$Bu-Salcyen] were prepared by the procedure of Jacobsen and characterized in the normal way.[31] The procedure for **1c**−**e** is the same as for **1a**,**b**.

***(R,R)*-[Cl-Salcyen] (1c).** Yield: 75%. $[\alpha]^D_0 = -508°$ ($c$ = 0.2, toluene). $^1$H NMR ($CDCl_3$, 250 MHz, 25 °C): $\delta$ 13.18 (s, 2H, O*H*), 8.17 (s, 2H, N=C*H*), 7.23 (dd, 2H, $^3J_{H-H}$ = 5.0 Hz $^4J_{H-H}$ = 2.4 Hz, Ar *H*), 7.15 (d, 2H, $^4J_{H-H}$ = 2.6 Hz, Ar *H*), 6.82 (d, 2H, $^3J_{HH}$ 8.8 Hz, Ar *H*), 3.31 (m, 2H, NC*H*), 1.94−1.68 (m, 4H, Cy *H*), 1.58−1.42 (m, 4H, Cy *H*). $^{13}$C NMR ($CDCl_3$, 63 MHz, 25 °C): $\delta$ 163.58 (s, N=*C*H), 159.50 (s, Ar $C_{ipso}$), 132.13 (s, Ar *C*), 130.53 (s, Ar *C*), 123.26 (s, Ar $C_{ipso}$), 119.28 (s, Ar $C_{ipso}$), 118.42 (s, Ar *C*), 72.65 (s, N*C*H), 32.92 (s, Cy *C*), 24.06 (s, Cy *C*). IR (Nujol mull; cm$^{-1}$): $\nu$(C=N), 1647 (s); $\nu$(C=C), 1633 (m). Anal. Calcd (found): C, 61.2 (61.3); H, 5.3 (5.1); N, 7.2 (7.2). MS: M − 1 at *m*/*e* 390.

***(R,R)*-[Br-Salcyen] (1d).** Yield: 83%. $[\alpha]^D_0 = -339°$ ($c$ = 0.1, toluene). $^1$H NMR ($CDCl_3$, 250 MHz, 25 °C): $\delta$13.21 (s, 2H, O*H*), 8.16 (s, 2H, N=C*H*), 7.32 (dd, 2H, $^3J_{H-H}$ = 4.9 Hz,

(30) Ward, C. V.; Mingliang, J.; Thornton-Pett, M.; Kee, T. P. *Tetrahedron Lett.*, in press.

(31) Larrow, J. F.; Jacobsen, E. N.; Gao, Y.; Hong, Y.; Nie, X.; Zepp, C. M. *J. Org. Chem*. **1994**, *59*, 1939.

$^4J_{H-H}$ = 2.6 Hz, Ar *H*), 7.25 (d, 2H, $^4J_{H-H}$ = 2.7 Hz, Ar *H*), 6.79 (d, 2H, $^3J_{H-H}$ = 8.8 Hz, Ar *H*), 3.30 (m, 2H, NC*H*), 1.96−1.68 (m, 4H, Cy *H*), 1.56−1.38 (m, 4H, Cy *H*). $^{13}$C NMR ($CDCl_3$, 63 MHz, 25 °C): $\delta$ 163.49 (s, N=*C*H), 159.99 (s, Ar $C_{ipso}$), 134.96 (s, Ar *C*), 133.53 (s, Ar *C*), 119.92 (s, Ar $C_{ipso}$), 118.89 (s, Ar *C*), 110.10 (s, Ar $C_{ipso}$), 72.66 (s, N*C*H), 32.94 (s, Cy *C*), 24.07 (s, Cy *C*). IR (Nujol mull; cm$^{-1}$): $\nu$(C=N), 1632 (s); $\nu$(C=C), 1570 (m). Anal. Calcd (found): C, 49.9 (50.0); H, 4.2 (4.2); N, 5.8 (5.8). MS: M − 1 at *m*/*e* 480

**(*R*,*R*)-[MeO-Salcyen] (1e).** Yield: 70%. $[\alpha]^D_0$ = −645.3° (*c* = 0.2, toluene). $^1$H NMR ($CDCl_3$, 250 MHz, 25 °C): $\delta$ 12.79 (s, 2H, O*H*), 8.19 (s, 2H, N=C*H*), 6.79 (m, 4H, Ar *H*), 6.59 (d, 2H, $^3J_{H-H}$ = 2.6 Hz, Ar *H*), 3.70 (s, 6H, OC$H_3$), 3.29 (m, 2H, NC*H*), 1.96−1.86 (m, 4H, Cy *H*), 1.51−1.46 (m, 4H, Cy *H*). $^{13}$C NMR ($CDCl_3$, 63 MHz, 25 °C): $\delta$ 164.47 (s, N=*C*H), 155.06 (s, Ar $C_{ipso}$), 151.13 (s, Ar $C_{ipso}$), 119.38 (s, Ar *C*), 118.24 (s, Ar $C_{ipso}$), 117.45 (s, Ar *C*), 114.83 (s, Ar *C*), 72.75 (s, N*C*H), 55.87 (s, *C*$H_3$O), 33.03 (s, Cy *C*), 24.15 (s, Cy *C*). IR (Nujol mull; cm$^{-1}$): $\nu$(C=N), 1631 (s); $\nu$(C=C), 1590 (m). Anal. Calcd (found): C, 68.9 (69.1); H, 6.9 (6.9); N, 7.4 (7.3). MS: M at *m*/*e* 382.

**(*R*,*R*)-[Salcyen]AlMe (2a).** (*R*,*R*)-[Salcyen] (0.95 g, 2.96 mmol) was dissolved in toluene (2 mL) under an inert atmosphere of dinitrogen. Trimethylaluminum (1.48 cm$^3$, 2.96 mmol) was injected dropwise over a period of 5 min, and the mixture was heated under reflux for 1 h. After it was cooled to ambient temperature, the product was collected by filtration as a yellow solid. Yield: 0.99 g (92%). $^1$H NMR ($CD_2Cl_2$, 250 MHz, 25 °C): $\delta$ 8.27 (d, 1 H, $^4J_{H-H}$ = 2.0 Hz, N=C*H*), 8.08 (d, 1 H, $^4J_{H-H}$ = 2.0 Hz, N=C*H*), 7.33 (m, 2 H, ArC*H*), 7.16 (m, 2 H, ArC*H*), 6.86 (m, 2 H, ArC*H*), 6.68 (m, 2 H, ArC*H*), 3.54 (m, 1 H, NC*H*), 3.03 (m, 1 H, NC*H*), 2.47 (m, 1 H, Cy *H*), 2.27 (m, 1 H, Cy *H*), 1.99 (m, 2 H, Cy *H*), 1.44−1.31 (m, 4 H, Cy *H*), −1.20 (s, 3 H, AlC$H_3$). $^{13}$C NMR ($CD_2Cl_2$, 63 MHz, 25 °C): $\delta$ 167.09 (s, N=*C*H), 166.71 (s), 166.54 (s, Ar $C_{ipso}$), 166.54 (s, Ar $C_{ipso}$), 161.68 (s, N=*C*H), 135.94 (s, Ar *C*), 135.03 (s, Ar *C*), 133.62 (s, Ar *C*), 133.07 (s, Ar *C*), 122.94 (s, Ar *C*), 121.61 (s, Ar *C*), 118.91 (s, Ar $C_{ipso}$), 118.69 (s, Ar $C_{ipso}$), 116.61 (s, Ar *C*), 116.12 (s, Ar *C*), 65.77 (s, N*C*H), 62.37 (s, N*C*H), 28.88 (s, Cy *C*), 26.99 (s, Cy *C*), 24.13 (s, Cy *C*), 23.74 (s, Cy *C*). IR (Nujol mull; cm$^{-1}$): $\nu$(C=N), 1632 (s); $\nu$(C=C), 1554 (m). Anal. Calcd (found): C, 69.50 (69.60); H, 6.50 (6.40); N, 7.80 (7.73). MS: M at *m*/*e* 363, (Salcyen)Al at *m*/*e* 347.

**(*R*,*R*)-[Salen-$^t$Bu]AlMe (2b).** (*R*,*R*)-[Salen-$^t$Bu] (0.5 g, 0.91 mmol) was dissolved in toluene (4 mL) under an inert atmosphere of dinitrogen. Trimethylaluminum (0.55 cm$^3$, 1.10 mmol) was injected dropwise to the stirred solution over a period of 5 min, and the mixture heated under reflux for 6 h. Removal of the volatiles under reduced pressure afforded the product as a yellow solid which was recrystallized from toluene at −35 °C. Yield: 0.15 g (29%). $[\alpha]^D_0$ = −457.6° (*c* = 1; THF). $^1$H NMR ($CDCl_3$; 250 MHz, 25 °C): $\delta$ 8.28 (d, 1H, $^4J_{H-H}$ = 1.5 Hz, N=C*H*), 8.11 (d, 1H, $^4J_{H-H}$ = 1.8 Hz, N=C*H*), 7.49 (dd, 2H, $^4J_{H-H}$ = 4.7 Hz, ArC*H*), 7.05 (d, 1H, $^4J_{H-H}$ = 2.6 Hz, ArC*H*), 6.97 (d, 1H, $^4J_{H-H}$ = 2.6 Hz, ArC*H*), 3.52 (m, 1H, NC*H*), 3.06 (m, 1H, NC*H*), 2.55 (m, 1H, Cy *H*), 2.39 (m, 1H, Cy *H*), 1.99 (m, 2H, Cy *H*), 1.55−1.35 (m, 4H, Cy *H*), 1.53 (s, 9H, C$H_3$), 1.52 (s, 9H, C$H_3$), 1.32 (s, 9H, C$H_3$), 1.30 (s, 9H, C$H_3$), −1.20 (s, 3H, AlC$H_3$). $^{13}$C NMR ($CDCl_3$, 63 MHz, 25 °C): $\delta$ 167.64 (s, N=*C*), 164.11 (s, Ar $C_{ipso}$), 162.53 (s, Ar $C_{ipso}$), 162.07 (s, N=*C*), 141.09 (s, Ar $C_{ipso}$), 141.00 (s, Ar $C_{ipso}$), 137.62 (s, Ar $C_{ipso}$), 137.07 (s, Ar $C_{ipso}$), 130.61 (s, Ar *C*), 129.69 (s, Ar *C*), 127.54 (s, Ar *C*), 127.19 (s, Ar *C*), 118.33 (s, Ar $C_{ipso}$), 118.27 (s, Ar $C_{ipso}$), 65.72 (s, N*C*H), 62.45 (s, N*C*H), 35.65 (s, *C*$(CH_3)_3$), 35.50 (s, *C*$(CH_3)_3$), 33.96 (s, *C*$(CH_3)_3$), 33.80 (s, *C*$(CH_3)_3$), 31.50 (s, *C*$H_3$), 31.40 (s, *C*$H_3$), 29.76 (s, *C*$H_3$), 29.65 (s, *C*$H_3$), 28.91 (s, Cy *C*), 27.26 (s, Cy *C*), 24.27 (s, Cy *C*), 23.82 (s, Cy *C*). Anal. Calcd (found): C, 74.90 (75.70); H, 9.75 (9.45); N, 4.55 (4.77). MS: ($^t$Bu-Salcyen)Al at *m*/*e* 571.

**(*R*,*R*)-[Cl-Salcyen]AlMe (2c).** The procedure was as for **2a**. Yield: 87%. $[\alpha]^D_0$ = −462° (*c* = 0.1, toluene). $^1$H NMR ($CD_2Cl_2$, 250 MHz, 25 °C): $\delta$ 8.21 (d, 1H, $^4J_{H-H}$ = 1.8 Hz, N=C*H*), 8.04 (d, 1H, $^4J_{H-H}$ = 1.8 Hz, N=C*H*), 7.33−7.02 (m, 6H, Ar *H*), 3.61 (m, 1H, NC*H*), 3.11 (m, 1H, NC*H*), 2.54 (m, 1H, Cy *H*), 2.37 (m, 1H, Cy *H*), 2.11 (m, 2H, Cy *H*), 1.57−1.26 (m, 4H, Cy *H*), −1.08 (s, 3H, AlC$H_3$). IR (Nujol mull; cm$^{-1}$): $\nu$(C=N), 1647 (s); $\nu$(C=C), 1633 (m). Anal. Calcd (found): C, 57.9 (58.5); H, 5.1 (4.9); N, 6.1 (6.5). MS: M ($^{35}$Cl) at *m*/*e* 430.

**(*R*,*R*)-[Br-Salcyen]AlMe (2d).** The procedure was as for **2a**. Yield: 72%. $^1$H NMR ($CD_2Cl_2$, 250 MHz, 25 °C): $\delta$ 8.21 (d, 1H, $^4J_{H-H}$ = 2.2, N=C*H*), 8.04 (d, 1H, $^4J_{H-H}$ = 2.2, N=C*H*), 7.45 (ddd, 2H, $^4J_{H-H}$ = 9 Hz, $^4J_{H-H}$ = 2.7 Hz, $^5J_{H-H}$ = 1.4 Hz, Ar *H*), 7.32 (dd, 2H, $^3J_{H-H}$ = 12.4 Hz, $^4J_{H-H}$ = 5 Hz, Ar *H*), 6.96 (dd, 2H, $^3J_{H-H}$ = 15.2 Hz, $^4J_{H-H}$ = 7.4 Hz, Ar *H*), 3.64 (m, 1H, NC*H*), 3.10 (m, 1H, NC*H*), 2.53 (m, 1H, Cy *H*), 2.36 (m, 1H, Cy *H*), 2.11 (m, 2H, Cy *H*), 1.50−1.24 (m, 4H, Cy *H*), −1.08 (s, 3H, AlC$H_3$). $^{13}$C NMR ($CD_2Cl_2$, 63 MHz, 25 °C): $\delta$ 168.51 (s, Ar $C_{ipso}$), 167.29 (s, N=*C*H), 164.77 (s, Ar $C_{ipso}$), 161.75 (s, N=*C*H), 139.28 (s, Ar *C*), 138.45 (s, Ar *C*), 136.17 (s, Ar *C*), 135.77 (s, Ar *C*), 124.85 (s, Ar *C*), 124.68 (s, Ar *C*), 121.28 (s, Ar $C_{ipso}$), 120.97 (s, Ar $C_{ipso}$), 108.29 (s, Ar $C_{ipso}$), 107.68 (s, Ar $C_{ipso}$), 66.76 (s, N*C*H), 63.39 (s, N*C*H), 29.72 (s, Cy *C*), 27.76 (s, Cy *C*), 24.89 (s, Cy *C*), 24.43 (s, Cy *C*), Al−*C*$H_3$ not located. IR (Nujol mull; cm$^{-1}$): $\nu$(C=N), 1629 (s); $\nu$(C=C), 1544 (m). Anal. Calcd (found): C, 48.3 (48.5); H, 4.0 (4.1); N, 5.1 (5.4). MS: M ($^{80}$Br) at *m*/*e* 520.

**(*R*,*R*)-[MeO-Salcyen]AlMe (2e).** The procedure was as for **2a**. Yield: 93%. $^1$H NMR ($CD_2Cl_2$, 250 MHz, 25 °C): $\delta$ 8.13 (d, 1H, $^4J_{H-H}$ = 1.3, N=C*H*), 7.97 (d, 1H, $^4J_{H-H}$ = 1.3, N=C*H*), 7.28−6.97 (m, 4H, Ar *H*), 6.59 (m, 2H, Ar *H*), 3.57 (m, 1H, NC*H*), 3.14 (m, 1H, NC*H*), 2.53 (m, 1H, Cy *H*), 2.35 (m, 1H, Cy *H*), 2.06 (m, 2H, Cy *H*), 1.64−1.23 (m, 4H, Cy *H*), −1.11 (s, 3H, AlC$H_3$). $^{13}$C NMR ($CD_2Cl_2$, 63 MHz, 25 °C): $\delta$ 166.49 (s, N=*C*H), 161.41 (s, N=*C*H), 161.32 (s, Ar $C_{ipso}$), 160.01 (s, Ar $C_{ipso}$), 150.34 (s, Ar *C*), 149.99 (s, Ar *C*), 134.46 (s, Ar $C_{ipso}$), 134.10 (s, Ar $C_{ipso}$), 123.75 (s, Ar *C*), 123.51 (s, Ar *C*), 117.82 (s, Ar $C_{ipso}$), 117.49 (s, Ar $C_{ipso}$), 114.75 (s, Ar *C*), 114.49 (s, Ar *C*), 65.45 (s, N*C*H), 62.45 (s, N*C*H), 55.98 (s, O*C*$H_3$), 55.93 (s, O*C*$H_3$), 28.89 (s, Cy *C*), 27.01 (s, Cy *C*), 24.10 (s, Cy *C*), 23.74 (s, Cy *C*). Al−*C*$H_3$ not located. IR (Nujol mull; cm$^{-1}$): $\nu$(C=N), 1630 (s); $\nu$(C=C), 1550 (m). Anal. Calcd (found): C, 65.1 (65.4); H, 6.5 (6.4); N, 6.3 (6.6). MS: M at *m*/*e* 421.

**(*R*,*R*)-[Salcyen]AlCl (4a).** (*R*,*R*)-[Salcyen] (8.6 g, 27 mmol) was dissolved in toluene (20 mL) under an inert atmosphere of dinitrogen. Chlorodimethylaluminum (27 mL, 27 mmol) in toluene (20 mL) was added dropwise over a period of 5 min, and the mixture was heated under reflux for 1 h. The yellow crystalline product was collected by vacuum filtration. Yield: 9.9 g (96%). $^1$H NMR ($CD_3OD$, 250 MHz, 25 °C): $\delta$ 8.69 (s, 2H, N=C*H*), 7.71−7.60 (m, 4H, ArC*H*), 7.18 (d, 2H, $^2J_{H-H}$ = 8.3 Hz, ArC*H*), 7.00 (dd, 2H, $^3J_{H-H}$ = 0.9 Hz, $^3J_{H-H}$ = 10.9 Hz, ArC*H*), 3.62 (m, 2H, NC*H*), 2.88 (m, 2H, Cy *H*), 2.28 (m, 2H, Cy *H*), 1.72 (m, 4H, Cy *H*). $^{13}$C NMR ($CD_3OD$, 63 MHz, 25 °C): $\delta$ 167.39 (s, N=*C*H), 165.83 (s, Ar $C_{ipso}$), 137.16 (s, Ar *C*), 136.05 (s, Ar *C*), 122.43 (s, Ar *C*), 121.76 (s, Ar *C*), 118.23 (s, Ar *C*), 65.13 (s, N*C*H), 28.38 (s, Cy *C*), 25.08 (s, Cy *C*). Anal. Calcd (found): C, 62.60 (62.70); H, 5.45 (5.27); N, 7.10 (7.73). MS: M at *m*/*e* 382, (Salcyen)Al at *m*/*e* 347.

**(*R*,*R*)-[$^t$Bu-Salcyen]AlCl (4b).** (*R*,*R*)-[$^t$Bu-Salcyen] (1 g, 1.82 mmol) was dissolved in toluene (6 mL) under a dinitrogen atmosphere and cooled to −78 °C. Chlorodimethylaluminum (2 mL, 2 mmol) was added dropwise with stirring over a period of 5 min. The mixture was then warmed to room temperature over 2 h and stirred for a further 10 h. Removal of the volatiles under reduced pressure afforded the pure product, which was recrystallized from toluene as a yellow solid. Yield: 1.09 g (99%). $[\alpha]^D_0$ = −376.8° (*c* = 1, MeOH). $^1$H NMR ($CD_3OD$, 250 MHz, 25 °C): $\delta$ 8.43 (s, 2H, N=C*H*), 7.54 (d, 2H, $^4J_{H-H}$ = 2.6 Hz, Ar *H*), 7.29 (d, 2H, $^4J_{H-H}$ = 2.6 Hz, Ar *H*), 3.28 (m, 2H, NC*H*), 2.68 (m, 2H, Cy *H*), 2.07 (m, 2H, Cy *H*), 1.55−1.35 (m, 4H, Cy *H*), 1.55 (s, 18H, C$H_3$), 1.30 (s, 18H, C$H_3$). $^{13}$C NMR ($CD_3OD$, 63 MHz, 25 °C): $\delta$ 167.87 (s, N=*C*H), 163.91 (s, Ar

$C_{ipso}$), 141.71 (s, Ar $C_{ipso}$), 139.74 (s, Ar $C_{ipso}$), 132.00 (s, Ar *C*), 130.51 (s, Ar *C*), 120.53 (s, Ar $C_{ipso}$), 65.42 (s, N*C*H), 37.03 (s, *C*$(CH_3)_3$), 35.39 (s, *C*$(CH_3)_3$), 32.30 (s, *C*$H_3$), 30.87 (s, *C*$H_3$), 28.77 (s, Cy *C*), 25.59 (s, Cy *C*). Anal. Calcd (found): C, 71.3 (71.2); H, 8.7 (8.6); N, 4.5 (4.6). MS: M − 1 at *m/e* 606.

**(*R,R*)-[Salcyen]AlOSi$^t$BuMe$_2$ (3a)**. (*R,R*)-[Salcyen]AlMe (**2a**; 100 mg, 0.28 mmol) was suspended in toluene (3 mL), and *tert*-butyldimethylsilanol (0.044 mL, 0.28 mmol) was added dropwise over a period of 5 min. After it was stirred for 2 days at 50 °C, the mixture was concentrated and cooled to −35 °C to afford the title compound as pale yellow crystals. Yield: 131 mg (98%). $[\alpha]^D_0 = -788°$ (*c* = 0.1, THF). $^1$H NMR ($CDCl_3$, 250 MHz, 25 °C): *δ* 8.28 (d, 1H, $^4J_{H-H}$ = 2.1 Hz, N=C*H*), 8.08 (d, 1H, $^4J_{H-H}$ = 2.1 Hz, N=C*H*), 7.39 (m, 2H, Ar *H*), 7.25−7.07 (m, 4H, Ar *H*), 6.74 (m, 2H, Ar *H*), 3.79 (m, 1H, NC*H*), 3.08 (m, 1H, NC*H*), 2.54 (m, 1H, Cy *H*), 2.40 (m, 1H, Cy *H*), 2.08 (m, 2H, Cy *H*), 1.45 (m, 4H, Cy *H*), 0.61 (s, 9H, C$H_3$), −0.37 (s, 3H, SiC$H_3$), −0.38 (s, 3H, SiC$H_3$). $^{13}$C NMR ($CDCl_3$, 63 MHz, 25 °C): *δ* 166.73 (s, N=*C*H), 166.52 (s, Ar $C_{ipso}$), 165.17 (s, Ar $C_{ipso}$), 161.69 (s, N=*C*H), 135.71 (s, N*C*H), 134.88 (s, N*C*H), 133.33 (s, Ar *C*), 132.86 (s, Ar *C*), 122.82 (s, Ar *C*), 122.68 (s, Ar *C*), 118.66 (s, Ar $C_{ipso}$), 188.65 (s, Ar $C_{ipso}$), 116.68 (s, Ar *C*), 116.18 (s, Ar *C*), 65.59 (s, N*C*H), 62.64 (s, N*C*H), 28.85 (s, Cy *C*), 27.00 (s, Cy *C*), 26.03 (s, C(*C*$H_3)_3$), 24.10 (s, Cy *C*), 23.84 (s, Cy *C*), 18.38 (s, *C*$(CH_3)_3$), −2.54 (s, Si*C*$H_3$), −2.61 (s, Si*C*$H_3$). IR (Nujol mull; $cm^{-1}$): *ν*(C=N), 1650 (s); *ν*(C=C), 1625 (m). Anal. Calcd (found): C, 64.9 (65.2); H, 7.3 (7.4); N, 5.6 (5.8). MS: M − 1 at *m/e* 477; M − $CH_3$ at *m/e* 463; M − $^t$Bu at *m/e* 421.

**(*R,R*)-[$^t$Bu-Salcyen]AlOSi$^t$BuMe$_2$ (3b).** The procedure was analogous to that of **3a**. Yield: 97%. $^1$H NMR ($CDCl_3$, 250 MHz, 25 °C): *δ* 8.30 (d, 1H, $^4J_{H-H}$ = 1.8 Hz, N=C*H*), 8.12 (d, 1H, $^4J_{H-H}$ = 1.5 Hz, N=C*H*), 7.49 (d, 2H, $^4J_{H-H}$ = 1.5 Hz, Ar *H*), 7.04 (d, 1H, $^4J_{H-H}$ = 2.8 Hz, Ar *H*), 7.00 (d, 1H, $^4J_{H-H}$ = 2.8 Hz, Ar *H*), 3.79 (m, 1H, NC*H*), 3.09 (m, 1H, NC*H*), 2.60 (m, 1H, Cy *H*), 2.43 (m, 1H, Cy *H*), 2.07 (m, 2H, Cy *H*), 1.55−1.35 (m, 4H, Cy *H*), 1.54 (s, 9H, C$H_3$), 1.53 (s, 9H, C$H_3$), 1.32 (s, 9H, C$H_3$), 1.30 (s, 9H, C$H_3$), −0.41 (s, 3H, SiC$H_3$), −0.42 (s, 3H, SiC$H_3$). $^{13}$C NMR ($CDCl_3$, 63 MHz, 25 °C): *δ* 167.09 (s, 2C, N=*C*H), 162.41 (s, 2C, Ar $C_{ipso}$), 140.72 (s, Ar $C_{ipso}$), 140.82 (s, Ar $C_{ipso}$), 137.73 (s, Ar $C_{ipso}$), 137.32 (s, Ar $C_{ipso}$), 130.39 (s, N*C*H), 129.62 (s, N*C*H), 127.16 (s, Ar *C*), 127.05 (s, Ar *C*), 118.22 (s, Ar $C_{ipso}$), 118.23 (s, Ar $C_{ipso}$), 65.55 (s, N*C*H), 62.78 (s, N*C*H), 35.63 (s, *C*$(CH_3)_3$), 35.55 (s, *C*$(CH_3)_3$), 33.96 (s, *C*$(CH_3)_3$), 33.92 (s, *C*$(CH_3)_3$), 31.45 (s, *C*$H_3$), 31.39 (s, 3C, *C*$H_3$), 29.99 (s, *C*$H_3$), 29.75 (s, *C*$H_3$), 28.91 (s, Cy *C*), 27.20 (s, Cy *C*), 26.10 (s, SiOC(*C*$H_3)_3$), 24.26 (s, Cy *C*), 24.02 (s, Cy *C*), 18.43 (s, SiO*C*$(CH_3)_3$), −2.55 (s, Si*C*$H_3$), −2.63 (s, Si*C*$H_3$). Anal. Calcd (found): C, 71.6 (71.8); H, 9.7 (9.6); N, 3.8 (4.0). MS: M − 1 at *m/e* 702; M − $CH_3$ at *m/e* 687; M − $^t$Bu at *m/e* 645.

**(*R,R*)-[Cl-Salen]AlOSiMe$_2$tBu (3c).** The procedure was analogous to that of **3a**. Yield: 83%. $[\alpha]^D_0 = -788°$ (*c* = 0.1, THF). $^1$H NMR ($CDCl_3$, 250 MHz, 25 °C): *δ* 8.19 (s, 1H, N=C*H*), 8.01 (s, 1H, N=C*H*), 7.34−6.99 (m, 6H, Ar *H*), 3.76 (m, 1H, NC*H*), 3.12 (m, 1H, NC*H*), 2.53 (m, 1H, Cy *H*), 2.35 (m, 1H, Cy *H*), 2.09 (m, 2H, Cy *H*), 1.47 (m, 4H, Cy *H*), 0.61 (s, 9H, C$H_3$), −0.38 (s, 3H, SiC$H_3$), −0.39 (s, 3H, SiC$H_3$). $^{13}$C NMR ($CDCl_3$, 63 MHz, 25 °C): *δ* 165.90 (s, N=*C*H), 164.91 (s, Ar $C_{ipso}$), 163.56 (s, Ar $C_{ipso}$), 160.92 (s, N=*C*H), 135.82 (s, Ar *C*), 134.95 (s, Ar *C*), 131.84 (s, Ar *C*), 131.57 (s, Ar *C*), 124.24 (s, Ar *C*), 124.14 (s, Ar *C*), 121.17 (s, Ar $C_{ipso}$), 120.59 (s, Ar $C_{ipso}$), 119.35 (s, Ar $C_{ipso}$), 119.07 (s, Ar $C_{ipso}$), 65.64 (s, N*C*H), 62.79 (s, N*C*H), 28.82 (s, Cy *C*), 26.97 (s, Cy *C*), 25.99 (s, SiOC(*C*$H_3)_3$), 24.02 (s, Cy *C*), 23.73 (s, Cy *C*), 18.36 (s, SiO*C*$(CH_3)_3$), −2.51 (s, Si*C*$H_3$), −2.58 (s, Si*C*$H_3$). IR (Nujol mull; $cm^{-1}$): *ν*(C=N), 1635 (s); *ν*(C=C), 1540 (m). Anal. Calcd (found): C, 57.4 (57.1); H, 5.9 (6.1); N, 5.0 (5.1). MS: M at *m/e* 545; M − $CH_3$ at *m/e* 531; M − $^t$Bu at *m/e* 489.

**(*R,R*)-[Br-Salcyen]AlOSiMe$_2$tBu (3d).** The procedure was analogous to that of **3a**. Yield: 89%. $[\alpha]^D_0 = -487.5°$ (*c* = 0.16, THF). $^1$H NMR ($CDCl_3$, 250 MHz, 25 °C): *δ* 8.18 (s, 1H, N=C*H*), 8.00 (s, 1H, N=C*H*), 7.45−6.92 (m, 6H, Ar *H*), 3.79 (m, 1H, NC*H*), 3.09 (m, 1H, NC*H*), 2.52 (m, 1H, Cy *H*), 2.33 (m, 1H, Cy *H*), 2.08 (m, 2H, Cy *H*), 1.45 (m, 4H, Cy *H*), 0.59 (s, 9H, C$H_3$), −0.39 (s, 3H, SiC$H_3$), −0.40 (s, 3H, SiC$H_3$). $^{13}$C NMR ($CDCl_3$, 63 MHz, 25 °C): *δ* 165.84 (s, N=*C*H), 164.50 (s, Ar $C_{ipso}$), 163.93 (s, Ar $C_{ipso}$), 160.83 (s, N=*C*H), 138.46 (s, Ar *C*), 137.66 (s, Ar *C*), 134.95 (s, Ar *C*), 134.63 (s, Ar *C*), 128.99 (s, Ar *C*), 128.19 (s, Ar *C*), 124.66 (s, Ar $C_{ipso}$), 124.55 (s, Ar $C_{ipso}$), 119.86 (s, Ar $C_{ipso}$), 107.31 (s, Ar $C_{ipso}$), 65.64 (s, N*C*H), 62.76 (s, N*C*H), 28.79 (s, Cy *C*), 26.95 (s, Cy *C*), 25.96 (s, SiOC(*C*$H_3)_3$), 23.99 (s, Cy *C*), 23.69 (s, Cy *C*), 18.32 (s, SiO*C*$(CH_3)_3$), −2.54 (s, Si*C*$H_3$), −2.61 (s, Si*C*$H_3$). IR (Nujol mull; $cm^{-1}$): *ν*(C=N), 1633 (s); *ν*(C=C), 1535 (m). Anal. Calcd (found): C, 49.3 (49.1); H, 5.0 (5.2); N, 4.2 (4.4). MS: M at *m/e* 635; M − $CH_3$ at *m/e* 621; M − $^t$Bu at *m/e* 579 (all $^{80}$Br).

**(*R,R*)-[MeO-Salcyen]AlOSiMe$_2$tBu (3e).** The procedure was analogous to that of **3a**. Yield: 90%. $[\alpha]^D_0 = -1120°$ (*c* = 0.2, THF). $^1$H NMR ($CDCl_3$, 250 MHz, 25 °C): *δ* 8.12 (s, 1H, N=C*H*), 7.95 (s, 1H, N=C*H*), 7.25−7.14 (m, 2H, Ar *H*), 7.09−6.98 (m, 2H, Ar *H*), 6.60 (dd, 2H, $^3J_{H-H}$ = 11.8 Hz, $^4J_{H-H}$ 2.7 Hz, Ar *H*), 3.76 (s, 3H, OC$H_3$), 3.74 (s, 3H, OC$H_3$), 3.68 (m, 1H, NC*H*), 3.07 (m, 1H, NC*H*), 2.49 (m, 1H, Cy *H*), 2.34 (m, 1H, Cy *H*), 2.05 (m, 2H, Cy *H*), 1.43 (m, 4H, Cy *H*), 0.59 (s, 9H, C$H_3$), −0.40 (s, 3H, SiC$H_3$), −0.41 (s, 3H, SiC$H_3$). $^{13}$C NMR ($CDCl_3$, 63 MHz, 25 °C): *δ* 165.84 (s, N=*C*H), 164.50 (s, Ar $C_{ipso}$), 163.93 (s, Ar $C_{ipso}$), 160.83 (s, N=*C*H), 138.46 (s, Ar *C*), 137.66 (s, Ar *C*), 134.95 (s, Ar *C*), 134.63 (s, Ar *C*), 128.99 (s, Ar *C*), 128.19 (s, Ar *C*), 124.66 (s, Ar $C_{ipso}$), 124.55 (s, Ar $C_{ipso}$), 119.86 (s, Ar $C_{ipso}$), 107.31 (s, Ar $C_{ipso}$), 65.64 (s, N*C*H), 62.76 (s, N*C*H), 28.79 (s, Cy *C*), 26.95 (s, Cy *C*), 25.96 (s, 3C, SiOC-(*C*$H_3)_3$), 23.99 (s, Cy *C*), 23.69 (s, Cy *C*), 18.32 (s, 3C, SiO*C*$(CH_3)_3$), −2.54 (s, Si*C*$H_3$), −2.61 (s, Si*C*$H_3$). IR (Nujol mull; $cm^{-1}$): *ν*(C=N), 1640 (s); *ν*(C=C), 1555 (m). Anal. Calcd (found): C, 62.3 (62.5); H, 7.5 (7.3); N, 5.1 (5.2). MS: M at *m/e* 537; M − $CH_3$ at *m/e* 523; M − $^t$Bu at *m/e* 481.

**Typical Procedure for Catalytic Phospho-Aldol Reactions.** Catalyst (0.02 mmol) was dissolved in deuterated solvent (0.4 $cm^3$ $d_8$-THF or $d_8$-toluene) and the solution cooled to −78 °C (dry ice/acetone). Aldehyde (1 mmol) and dimethyl H-phosphonate (1 mmol) were added, and the mixture was warmed to room temperature over a period of 25 min. The sample was shaken to ensure homogeneity before being transferred to an NMR tube, where reaction progress was monitored by $^{31}$P NMR spectroscopy over a suitable time period (commonly 4 h).

**Determination of Enantiomeric Excesses of α-Hydroxyphosphonate Esters.** Following confirmation via $^{31}$P NMR spectroscopy for a reaction between dimethyl H-phosphonate and benzaldehyde 4 molar equiv of (−)-quinine was added to the NMR sample. Analysis of the $^{31}$P NMR spectrum revealed resonances for the twin diastereoisomeric complexes formed between *R* and *S* enantiomers of product phosphonate esters and (−)-quinine. Expansion of this region of the spectrum (ca. 20−25 ppm) allowed subsequent integration and direct measurement of ee.

**Configurational Stability of α-Hydroxyphosphonate Esters.** $(MeO)_2P(O)CHPh(OH)$ (30 mg, 0.14 mmol) and [Salen]-AlMe (50 mg, 0.14 mmol) were dissolved in deuterated methanol under aerobic conditions. The mixture was observed at regular intervals by $^1$H NMR spectroscopy. Integration of the methoxy proton resonances and methine proton resonances should, in the absence of racemizing methane group H/D exchange, afford a ratio of 6:1. Over the course of 4 days no evidence for incorporation of deuterium at this site was observed.

Subsequently, $(MeO)_2P(O)CHPh(OH)$ (0.92 mmol, 200 mg), 4-bromobenzaldehyde (0.92 mmol, 170 mg), and the Salcyen complexes **2a**,**b** (0.046 mmol) were dissolved in THF (2 $cm^3$), and the mixture was at room temperature for 5 days. Solvent was then removed by blowing dinitrogen directly onto the solvent surface; the crude product was redissolved in deuter-

ated $CDCl_3$ and analyzed via $^{31}P$ NMR spectroscopy. No products of aldehyde crossover were observed. The same experiment performed in the presence of $NEt_3$ (1 equiv) resulted in less than 2% crossover product.

Two reactions were performed simultaneously. **2a** (18.1 mg, 0.05 mmol) was dissolved in THF (1.8 $cm^3$) and cooled to −78 °C using a cardice/acetone slush bath. Dimethyl H-phosphonate (0.09 $cm^3$, 1 mmol) was injected and the mixture warmed to room temperature over a period of 25 min. After cooling to −78 °C, benzaldehyde (0.1 $cm^3$, 1 mmol) was injected and the sample shaken briefly to ensure a homogeneous mixture before being warmed to room temperature. After 24 h, one preparation was taken aside and the solvent removed by blowing dinitrogen directly onto the solvent surface to yield phosphonate ester product. The enantiomeric excess of this product was measured using quinine. After 8 days, the solvent from the second solution was removed and the enantiomeric excess of the phosphonate ester product again measured using quinine. In both cases, the results were identical.

$(MeO)_2P(O)CHPh(OH)$ (20 mg, 0.09 mmol) was dissolved in $CDCl_3$ (0.6 $cm^3$) containing quinine (120 mg, 0.37 mmol) in a 5 mm NMR tube and shaken briefly to ensure a homogeneous mixture. Integration of $^{31}P$ NMR resonances revealed an enantiomeric excess of 30% for the phosphonate ester. The NMR solution was allowed to stand in air for 5 days. Subsequent reanalysis revealed no evidence for quinine-catalyzed racemization of α-hydroxyphosphonate ester; the ee remained unchanged.

**Kinetic Analysis of the Phospho-Aldol Reaction.** Under an atmosphere of dry dinitrogen, the catalyst (0.02 mmol) was dissolved in deuterated solvent (0.4 $cm^3$; $C_7D_8$) and the solution transferred to a 5 mm NMR tube. After the mixture was cooled to −78 °C using a cardice/acetone slush bath, aldehyde (1 mmol) and dimethyl H-phosphonate (1 mmol) were injected. The sample was then warmed to −30 °C and shaken to ensure homogeneity before being introduced into the NMR spectrometer probe and warmed to 25 °C. The reaction was then monitored automatically by $^{31}P$ NMR using Bruker WINNMR software control, a spectrum being recorded every 30 min until reaction was >90% complete. Reactions were all fully $^1H$-coupled and had extended delay times between pulses to negate possible distorting NOE and relaxation effects in the integrations of DMHP at $\delta_P$ 10−11 ppm and product phosphonate ester at $\delta_P$ 22−25 ppm depending upon solvent. Data have been analyzed according to putative second-order kinetics using the equation $k_2t = x/([A_0] - x)[A_0]$, where $x$ is the degree of reaction and $[A_0]$ denotes the initial concentrations of both DMHP and aldehyde.

**Single-Crystal X-ray Diffraction Determinations.** All crystallographic measurements for each of the four complexes were made on a Nonius KappaCCD area-detector diffractometer using molybdenum Kα radiation ($\lambda$ = 0.710 73 Å). All four data sets were corrected for absorption empirically using redundant and symmetry-related reflections.[32] All four structures were solved by direct methods using SHELXS-86[33] and were refined by full-matrix least squares (against all $F^2$ data) using SHELXL-93.[34] All non-hydrogen atoms of each complex (including those of the solvent cocrystallites of **2a** and **3a**,**e**) were refined with anisotropic displacement parameters. Hydrogen atoms were constrained to idealized positions using a riding model with the exception of the OH hydrogen atoms of the coordinated methanol molecules of **4b**, which were located on a Fourier difference synthesis and freely refined. The chirality of compounds **2a**, **3e**, and **4b** was confirmed by refinement of a Flack enantiopole parameter.[35] Crystal data and details of data collection and structure refinement are listed in Table 2. Further details are included in the Supporting Information.

**Acknowledgment.** We thank the EPSRC, the European Coal and Steel Community (grant #7220-PR-049), and the China Scholar Council for their support of J.P.D., J.N.D.W., and M.J., respectively. Thanks are due also to Sylvain Tredan and Mickaël Demay (Institute Universitaire de Technologie, Lannion, France) for valuable synthetic contributions, to Colin Kilner for X-ray data collection on **3e**, and to Albright and Wilson Ltd. and Zeneca Pharmaceuticals Ltd. for partial support of this work. Finally, we are most grateful to Professor David Atwood (University of Kentucky) for his valuable comments and advice.

**Supporting Information Available:** X-ray data for **2a**, **3a**,**e**, and **4b**, including tables of fractional coordinates and isotropic thermal parameters, anisotropic thermal parameters, interatomic distances, and intramolecular angles, experimental kinetic data for the reactions between H-phosphonates and benzaldehydes, and tables giving phospho-aldol turnover numbers of different solvents, ee's of phospho-aldol reactions catalyzed by **3a**−**e**, and phospho-aldol turnover numbers when catalyzed by **3a**−**e**, and a Hammett plot of $\log(ee_{Ar}/ee_{Ph})$ vs $\sigma_p$ and ee's of the phospho-aldol reaction catalyzed by **2b**. This material is available free of charge via the Internet at http://pubs.acs.org.

OM000386M

(32) Blessing, R. H. *Acta Crystallogr., Sect. A* **1995**, *51*, 33.
(33) Sheldrick, G. M. *Acta Crystallogr., Sect. A* **1990**, *46*, 467.
(34) Sheldrick, G. M. SHELXL 93, Program for Refinement of Crystal Structures; University of Göttingen, Göttingen, Germany, 1993.
(35) Flack, H. D. *Acta Crystallogr., Sect. A* **1983**, *39*, 876.